Fulling-Davies-Unruh effect for accelerated two-level single and entangled atomic systems

Arnab Mukherjee[*], Sunandan Gangopadhyay,[†] and Archan S. Majumdar[‡]

Department of Astrophysics and High Energy Physics, S.N. Bose National Centre for Basic Sciences, JD Block, Sector III, Salt Lake, Kolkata 700106, India

We investigate the transition rates of uniformly accelerated two-level single and entangled atomic systems in empty space as well as inside a cavity. We take into account the interaction between the systems and a massless scalar field from the viewpoint of an instantaneously inertial observer and a coaccelerated observer, respectively. The upward transition occurs only due to the acceleration of the atom. For the two-atom system, we consider that the system is initially prepared in a generic pure entangled state. In the presence of a cavity, we observe that for both the single and the two-atom cases, the upward and downward transitions are occurred due to the acceleration of the atomic systems. The transition rate manifests subtle features depending upon the cavity and system parameters, as well as the initial entanglement. It is shown that no transition occurs for a maximally entangled superradiant initial state, signifying that such entanglement in the accelerated two-atom system can be preserved for quantum information processing applications. Our analysis comprehensively validates the equivalence between the effect of uniform acceleration for an inertial observer and the effect of a thermal bath for a coaccelerated observer, in free space as well as inside a cavity, if the temperature of the thermal bath is equal to the Unruh temperature.

I. INTRODUCTION

Relativistic quantum information is a growing area of study that combines ideas from gravitational physics with those from quantum information theory [1–6]. From the perspective of quantum communications, the fundamental role herein is played by quantum entanglement [7]. In recent times one of the key prototypes in research on entangled states in the relativistic domain are systems of two-level atoms interacting with quantum fields [8,9]. Radiative processes of entangled states have been extensively discussed in the literature [10]. In this regard, several important works were developed [11–17], which establish important results concerning entanglement generation between two localized causally disconnected atoms. On the other hand, many investigations of atomic systems were also implemented on a curved background [18–21].

Quantum field theory in curved background is another important area of theoretical physics that predicts observation is a frame dependent entity. As an example, one can consider that a uniformly accelerated particle detector sees the Minkowski vacuum as a thermal bath with temperature T related to its proper acceleration α, given by $T = \alpha/2\pi$. This phenomenon arises as a result of the interaction between the detector and the fluctuating vacuum scalar fields, and is known as the Fulling-Davies-Unruh (FDU) effect [22–25]. After the seminal works of Fulling-Davies-Unruh [22–24], research into this phenomenon have been extended to include how a particle detector interacts with different quantum fields [26–41]. The application of both classical and quantum field theory has greatly improved the understanding of the origin of such phenomena [27]. In addition to being significant, the FDU effect is also connected to a number of current research areas, including thermodynamics and the information paradox of a black hole [24,42–44].

There are several theoretical provisions for possible observable manifestations of the FDU effect. In particular, it has been theoretically realized that when a uniformly accelerated single particle detector interacts with the vacuum massless scalar field, the spontaneous excitation rate of the accelerated detector is exactly same as seen by a locally inertial observer and by a coaccelerated observer. This equivalence is found to be true theoretically both in free space as well as in the presence of a reflecting boundary only if there exists a thermal bath at the FDU temperature in the coaccelerated frame [39]. Investigations on the radiative properties of a single uniformly accelerated atom [34–40] have also been extended to the scenarios where more than one atom is in interaction with the massless scalar field and the electromagnetic field [18,45–53].

Through the use of trapped atoms in optical nanofibers [54,55] and novel nanofabrication techniques [56,57], it is

[*]arnab.mukherjee@bose.res.in
[†]sunandan.gangopadhyay@bose.res.in
[‡]archan@bose.res.in

now possible to experimentally realize atomic excitations in nanoscale waveguides [58]. The examination of fundamental quantum optical concepts like atom-photon lattices is made possible by these pathways [59]. Studies on relativistic quantum phenomena in superconducting circuits [60,61] and secure quantum communication over long distances [62–65] highlight the significance of reflecting boundaries. Reflecting boundaries also play an important physical role in the context of quantum entanglement 69–66]], holographic entanglement entropy [70], atom-field interaction [71], and quantum thermodynamics [72].

The basic motivation of investigating the role of reflecting boundaries lies in its applicability to cavity quantum electrodynamics, a focus of fundamental research with numerous applications [73]. It has been observed that the resonance interatomic energy of two uniformly accelerated atoms can be effected due to the presence of boundaries [49,52,74] and noninertial atomic motion [47]. To study the Unruh-Davies effect inside cavities, techniques of cavity quantum electrodynamics can be used [75,76]. Additionally, cavity quantum electrodynamical configurations such as superconducting circuits [61] and laser-driven technologies [77–79] can achieve significant acceleration which is desirable for experimental verification of the theoretical results. Several theoretical analyses of the radiative processes of entangled atoms have been done by taking boundaries into account [66–69,75,76,80,81].

In a recent work [82], it has been found that there is an equivalence between the transition probabilities of an entangled two-atom system as observed by a Minkowski observer, and that by a coaccelerated observer in free space when the two-atom system is placed in a thermal bath. This equivalence only holds if the temperature of the thermal bath in the coaccelerated frame is taken to be equal to the Unruh temperature. However, this equivalence breaks down in general. On the other hand, it has also been found that the resonance interaction energy of a two-atom system as observed by an inertial observer and by a coaccelerated observer is the same in free space without considering any thermal bath at the Unruh temperature in the coaccelerated frame [48].

The above results, with certain seemingly conflicting implications, motivate us to perform a comprehensive investigation within the same framework involving the status of the FDU effect for both single and two-atomic entangled and accelerated systems in free space as well as in the presence of reflecting boundaries. Further motivation for our study in the context of cavities is two-fold. First of all, it is not clear *a priori*, whether such an equivalence will still hold inside a cavity. The reason for this is the following. The physics inside a cavity is significantly different from that in free space since a number of field modes are curtailed due to boundary conditions. The second reason for carrying our investigation inside a cavity is that the cavity set-up is more realistic from an experimental point of view. Several recent experiments have been done using cavity setup [56,57,83–85].

In the present work we consider the interaction between the atomic systems and a massless scalar field in the frame of an instantaneously inertial observer and a coaccelerated observer, respectively. The two-atom system is initially prepared in a generic pure entangled state. In the presence of a cavity, we show that for both the single and the two-atom cases, the magnitude of the upward and downward transitions increase due to the acceleration of the atomic systems. The transition rate displays interesting features with variation of the cavity and system parameters, as well as the initial entanglement. We find that no transition occurs for a maximally entangled superradiant initial state, indicating that such entanglement in the accelerated two-atom system can be preserved for quantum information processing applications. We further compute values of the transition rate for two examples using realistic cavity and system parameters. From our analysis it follows that the equivalence between the effect of uniform acceleration for an inertial observer and the effect of a thermal bath for a coaccelerated observer, holds in free space as well as inside a cavity, if the temperature of the thermal bath is set equal to the Unruh temperature.

The paper is organized as follows: In Sec. II, we recapitulate the basic framework for obtaining the transition rate when a single accelerated atom interacts with a massless scalar field. In Sec. III, we calculate the transition rates of the single atom from the viewpoint of the instantaneously inertial observer for empty space and in the presence of a cavity, respectively. A similar calculation of the transition rates of the single atom from the viewpoint of the coaccelerated observer for empty space and in the presence of a cavity, respectively, is presented in Sec. IV. We next consider the case of an entangled and accelerated two-atom system from Sec. V onward. In Sec. VI, we study this system from the point of view of an inertial observer. Subsequently, in Sec. VII we calculate the transition rate in context of the above system in context of a co-accelerated observer. We present a summary of our obtained results in Sec. VIII. Throughout the paper, we take $\hbar = c = k_B = 1$, where k_B is the Boltzmann constant.

II. COUPLING OF A SINGLE ATOM WITH A MASSLESS SCALAR FIELD

Let us consider a single atom with two energy levels, $-\omega_0/2$ and $+\omega_0/2$, traveling in vacuum with massless scalar field fluctuations. In the laboratory frame, trajectories of the atom can be represented through $x(\tau) = (t(\tau), \mathbf{x}(\tau))$. In the instantaneous inertial frame, the Hamiltonian describing the atom-field interaction in the interaction picture is given by [86]

$$H = \lambda m(\tau)\phi(x(\tau)), \tag{1}$$

where λ is the coupling constant which is assumed to be very small. The mode expansion of the massless scalar field reads [87]

$$\phi(x(\tau)) = \frac{1}{(2\pi)^{3/2}} \int_{-\infty}^{+\infty} \frac{d^3\mathbf{k}}{\sqrt{2\omega_{\mathbf{k}}}} [a_{\mathbf{k}} e^{-i\omega_{\mathbf{k}} t + i\mathbf{k}\cdot\mathbf{x}} + a_{\mathbf{k}}^{\dagger} e^{i\omega_{\mathbf{k}} t - i\mathbf{k}\cdot\mathbf{x}}] \tag{2}$$

where $k = (\omega_{\mathbf{k}}, \mathbf{k})$ is the four momentum and $\mathbf{k}$ is the three momentum. The monopole operator at any proper time τ of a single atom $m(\tau)$ is given by

$$m(\tau) = e^{iH_0\tau} m(0) e^{-iH_0\tau} \tag{3}$$

with $m(0) = |g\rangle\langle e| + |e\rangle\langle g|$ being the initial monopole operator and $H_0 = \epsilon|e\rangle\langle e|$ being the free Hamiltonian of a single atom respectively [72].

According to the time-dependent perturbation theory in the first-order approximation, the transition amplitude for the atom-field system from the initial atom-field state $|i\rangle \otimes |0_M\rangle \equiv |i, 0_M\rangle$ to the final atom-field state $|f, \phi_f\rangle$ is

$$\mathcal{A}_{|i,0_M\rangle \to |f,\phi_f\rangle} = i\lambda\langle f, \phi_f| \int_{-\infty}^{+\infty} m(\tau)\phi(x(\tau))|i, 0_M\rangle \tag{4}$$

where $|i\rangle$ and $|f\rangle$ are the initial and final atomic states whereas $|0_M\rangle$ and $|\phi_f\rangle$ are the initial (Minkowski vacuum state) and final field states. Now, squaring the above transition amplitude and summing over all possible field states, transition probability from the initial state $|i\rangle$ to the final state $|f\rangle$ can be written as

$$\mathcal{P}_{|i\rangle \to |f\rangle} = \lambda^2 |m_{fi}|^2 F(\Delta E), \tag{5}$$

where $\Delta E = E_f - E_i$, $m_{fi} = \langle f|m(0)|i\rangle$ and the response function $F(\Delta E)$ is defined as

$$F(\Delta E) = \int_{-\infty}^{+\infty} d\tau \int_{-\infty}^{+\infty} d\tau' e^{-i\Delta E(\tau-\tau')} G^+(x(\tau), x(\tau')) \tag{6}$$

with

$$G^+(x(\tau), x(\tau')) = \langle 0_M|\phi(x(\tau))\phi(x(\tau'))|0_M\rangle \tag{7}$$

being the positive frequency Wightman function of the massless scalar field [25]. Exploiting the time translational invariance property of the positive frequency Wightman function, the response function per unit proper time can be written as

$$\mathcal{F}(\Delta E) = \int_{-\infty}^{+\infty} d(\Delta\tau) e^{-i\Delta E\Delta\tau} G^+(x(\tau), x(\tau')) \tag{8}$$

where $\Delta\tau = \tau - \tau'$. Therefore, transition probability per unit proper time from the initial state $|i\rangle$ to the final state $|f\rangle$ turns out to be

$$\mathcal{R}_{|i\rangle \to |f\rangle} = \lambda^2 |m_{fi}|^2 \mathcal{F}(\Delta E). \tag{9}$$

In the following sections, the above formalism is used to examine the rate of transitions of a single atom under various conditions such as non-inertial motion of the atom, nature of the observer, type of the background field and the presence of a cavity.

III. TRANSITION RATES OF A SINGLE ATOM FROM THE VIEWPOINT OF A LOCAL INERTIAL OBSERVER

In this section, we study the transitions of a uniformly accelerated single atom interacting with a massless scalar field from the perspective of a locally inertial observer. To see the boundary effects on the transitions of the uniformly accelerated single atom in this scenario, several cases have been studied in the following subsections.

A. Transition rates in empty space with respect to a local inertial observer

We first evaluate the transition rates of a single atom that has been uniformly accelerated while interacting with a vacuum massless scalar field in the absence of any perfectly reflecting boundary. In the laboratory frame, the atomic trajectory is given by

$$t(\tau) = \frac{1}{\alpha}\sinh(\alpha\tau), \quad x(\tau) = \frac{1}{\alpha}\cosh(\alpha\tau), \quad y = z = 0, \tag{10}$$

where α and τ denote the proper acceleration and the proper time of the atom. Using the scalar field operator Eq. (2) in Eq. (7), the Wightman function becomes [25]

$$G^+(x(\tau), x(\tau')) = -\frac{1}{4\pi^2} \frac{1}{(t(\tau) - t(\tau') - i\epsilon)^2 - (x(\tau) - x(\tau'))^2 - (y(\tau) - y(\tau'))^2 - (z(\tau) - z(\tau'))^2}, \tag{11}$$

where ϵ is a small positive number. Substituting Eq. (10) in Eq. (11), the Wightman function turns out to be

$$G^+(x(\tau), x(\tau')) = -\frac{\alpha^2}{16\pi^2} \frac{1}{\sinh^2[\frac{1}{2}(\alpha\Delta\tau - i\epsilon)]}. \tag{12}$$

Substituting the Wightman function into Eqs. (8) and (9), the transition rate from the initial state $|i\rangle$ to the final state $|f\rangle$ becomes

$$
\mathcal{R}_{|i\rangle \to |f\rangle} = -\frac{\lambda^2 |m_{fi}|^2 \alpha^2}{16\pi^2} \int_{-\infty}^{+\infty} d(\Delta\tau) e^{-i\Delta E \Delta\tau}
$$
$$
\times \frac{1}{\sinh^2[\frac{1}{2}(\alpha\Delta\tau - i\varepsilon)]}. \tag{13}
$$

Simplifying the transition rates, Eq. (13), by performing the contour integration [88] as shown in Appendix A, we obtain

$$
\mathcal{R}_{|i\rangle \to |f\rangle} = \frac{\lambda^2 |m_{fi}|^2 |\Delta E|}{2\pi} \left[\theta(-\Delta E) \left(1 + \frac{1}{\exp(2\pi|\Delta E|/\alpha) - 1} \right) \right.
$$
$$
\left. + \theta(\Delta E) \left(\frac{1}{\exp(2\pi\Delta E/\alpha) - 1} \right) \right] \tag{14}
$$

where $\theta(\Delta E)$ is the Heaviside step function defined as

$$
\theta(\Delta E) = \begin{cases} 1, & \Delta E > 0, \\ 0, & \Delta E < 0. \end{cases} \tag{15}
$$

The above equation Eq. (14) reveals that two transition processes, namely upward and downward transition can take place when the atom is under uniform acceleration. Considering the initial state $|i\rangle = |g\rangle$, final state $|f\rangle = |e\rangle$ and vice-versa, and using the definition $m_{eg} = \langle e|m(0)|g\rangle$, we obtain $|m_{ge}|^2 = |m_{eg}|^2 = 1$, and $\Delta E = \omega_0$ for the transition $g \to e$ and $\Delta E = -\omega_0$ for the transition $e \to g$, respectively. Using the above results the upward and downward transition rates take the form

$$
\mathcal{R}_{|g\rangle \to |e\rangle} = \frac{\lambda^2 \omega_0}{2\pi} \left(\frac{1}{\exp(2\pi\omega_0/\alpha) - 1} \right) \tag{16}
$$
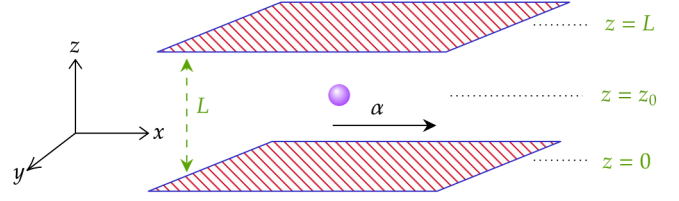

FIG. 1. Uniformly accelerated atom confined in a cavity.

$$
\mathcal{R}_{|e\rangle \to |g\rangle} = \frac{\lambda^2 \omega_0}{2\pi} \left(1 + \frac{1}{\exp(2\pi\omega_0/\alpha) - 1} \right). \tag{17}
$$

The upward transition in free space occurs solely due to the acceleration of the atom and vanishes in the limit $\alpha \to 0$. Taking the ratio of the above two results, we get

$$
\frac{\mathcal{R}_{|g\rangle \to |e\rangle}}{\mathcal{R}_{|e\rangle \to |g\rangle}} \equiv \frac{\mathcal{R}_{\text{up}}}{\mathcal{R}_{\text{down}}} = \exp\left(-2\pi\omega_0/\alpha\right). \tag{18}
$$

From the above expression, it is seen that the ratio of the upward and the downward transition rates depend only on the atomic acceleration and in the limit $\alpha \to \infty$, the ratio $\exp\left(-2\pi\omega_0/\alpha\right) \to 1$, and hence, the two transition rates are equal in this limit.

B. Transition rates in a cavity with respect to a local inertial observer

We now consider that a uniformly accelerated atom interacts with a vacuum massless scalar field confined to a cavity having length L (see Fig. 1). Assuming the scalar field obeys the Dirichlet boundary condition $\phi|_{z=0} = \phi|_{z=L} = 0$, and using the method of images, the positive frequency Wightman function of the vacuum massless scalar field confined to the cavity of length L takes the form [25]

$$
G^+(x(\tau), x(\tau')) = -\frac{1}{4\pi^2} \sum_{n=-\infty}^{\infty} \left[\frac{1}{(t(\tau) - t(\tau') - i\varepsilon)^2 - (x(\tau) - x(\tau'))^2 - (y(\tau) - y(\tau'))^2 - (z(\tau) - z(\tau') - nL)^2} \right.
$$
$$
\left. - \frac{1}{(t(\tau) - t(\tau') - i\varepsilon)^2 - (x(\tau) - x(\tau'))^2 - (y(\tau) - y(\tau'))^2 - (z(\tau) + z(\tau') - nL)^2} \right] \tag{19}
$$

with ε is a small positive number. To represent the atomic trajectories in terms of the atomic proper time τ, we choose the Cartesian coordinates in the laboratory frame so that the boundaries are fixed at $z = 0$ and $z = L$.

Inside the cavity the atomic trajectory is given by

$$
t(\tau) = \frac{1}{\alpha}\sinh(\alpha\tau), \qquad x(\tau) = \frac{1}{\alpha}\cosh(\alpha\tau), \qquad y = 0, \qquad z = z_0. \tag{20}
$$

Using the above trajectories in Eq. (19), the Wightman function becomes

$$G^+(x(\tau), x(\tau')) = -\frac{\alpha^2}{16\pi^2} \sum_{n=-\infty}^{\infty} \left[\frac{1}{\sinh^2[\frac{1}{2}(\alpha\Delta\tau - i\varepsilon)] - \frac{1}{4}d_1^2\alpha^2} - \frac{1}{\sinh^2[\frac{1}{2}(\alpha\Delta\tau - i\varepsilon)] - \frac{1}{4}d_2^2\alpha^2} \right] \tag{21}$$

with $d_1 = nL, d_2 = 2z_0 - nL$.

Now following the procedure in Appendix B, we finally obtain the upward and downward transition rates to be[1]

$$\mathcal{R}_{|g\rangle \to |e\rangle} = \lambda^2 \left[\left\{ \frac{\omega_0}{2\pi} + \mathfrak{f}\left(\omega_0, \alpha, \frac{L}{2}\right) - \mathfrak{h}\left(\omega_0, \alpha, z_0, \frac{L}{2}\right) \right\} \left(\frac{1}{\exp(2\pi\omega_0/\alpha) - 1} \right) \right] \tag{22}$$

$$\mathcal{R}_{|e\rangle \to |g\rangle} = \lambda^2 \left[\left\{ \frac{\omega_0}{2\pi} + \mathfrak{f}\left(\omega_0, \alpha, \frac{L}{2}\right) - \mathfrak{h}\left(\omega_0, \alpha, z_0, \frac{L}{2}\right) \right\} \left(1 + \frac{1}{\exp(2\pi\omega_0/\alpha) - 1} \right) \right]. \tag{23}$$

Note that the ratio of the upward and the downward transition rates in the cavity scenario is identical with the free space result [Eq. (18)].

Next, in order to describe the single boundary and free space cases, we take the limiting cases of the above expressions. Taking the limit $L \to \infty$, we find that in Eqs. (22) and (23) only the $n = 0$ term survives from the infinite summation terms, and one can effectively reduce the cavity scenario to a situation where only one reflecting boundary exists. Hence, using this limit, the upward and downward transition rates in the presence of a single reflecting boundary turn out to be[2]

$$\mathcal{R}_{|g\rangle \to |e\rangle} = \lambda^2 \left[\left\{ \frac{\omega_0}{2\pi} - \mathfrak{g}(\omega_0, \alpha, z_0) \right\} \left(\frac{1}{\exp(2\pi\omega_0/\alpha) - 1} \right) \right] \tag{24}$$

$$\mathcal{R}_{|e\rangle \to |g\rangle} = \lambda^2 \left[\left\{ \frac{\omega_0}{2\pi} - \mathfrak{g}(\omega_0, \alpha, z_0) \right\} \left(1 + \frac{1}{\exp(2\pi\omega_0/\alpha) - 1} \right) \right]. \tag{25}$$

The above results resemble those of the single boundary results obtained in [34,35] using the formalism developed by Dalibard, Dupont-Roc, and Cohen-Tannoudji [89,90].

On the other hand, taking the limits $L \to \infty$ and $z_0 \to \infty$ together, Eqs. (22) and (23) lead to the expression for the upward and downward transition rates in the free space given by Eqs. (16) and (17).

We now investigate the variation of the transition rate of a single two level atom (from its ground state energy level $|g\rangle$ to the excited state energy level $|e\rangle$) confined to a cavity with the length of the cavity (L), distance of the atom from the boundary (z_0), and the atomic acceleration (α). The findings are plotted below, where all physical quantities are expressed in dimensionless units.

Figure 2 shows the variation of the transition rate from $|g\rangle \to |e\rangle$ (per unit $\frac{\lambda^2\omega_0}{2\pi}$) with respect to the length of the cavity (separation between the two boundaries) for different values of distance of the atom from one boundary. From the plots, it can be seen that for a fixed value of the initial atomic distance z_0 from one boundary, the transition rate get enhanced when the cavity length increases and attains a maximum value for large values of L ($\omega_0 L \gg \omega_0 z_0$). This is expected since more number of field modes take part in the interaction between the scalar field and the atom after increasing the cavity length, which in turn increases the transition rate. When $\omega_0 L \gg \omega_0 z_0$, the cavity scenario reduces to the case of a single boundary, and hence, the upward transition rate reaches a constant value. It is also observed that the upper value of the rate is more for a larger value of $\omega_0 z_0$.

Figure 3 shows the variation of the transition rate from $|g\rangle \to |e\rangle$ (per unit $\frac{\lambda^2\omega_0}{2\pi}$) with respect to the distance of the atom from one boundary for different values of the length of the cavity, for a fixed value of acceleration. From the plots, it is observed that for a fixed value of the length of the cavity L, when we increase the atomic distance from one boundary, transition rate shows an oscillatory behavior and vanishes if either the atom touches any one of the boundaries or if the atom is equidistant from both boundaries. It can also be observed (as we have seen earlier in
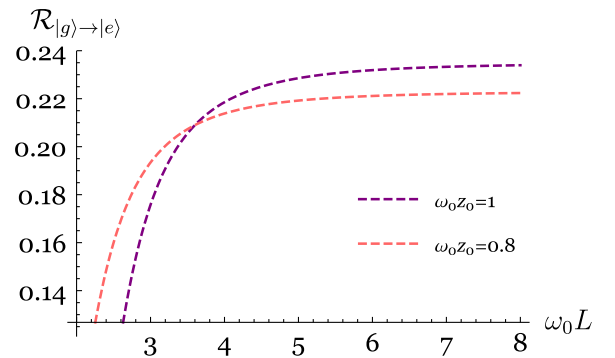

FIG. 2. Transition rate from $|g\rangle \to |e\rangle$ (per unit $\frac{\lambda^2\omega_0}{2\pi}$) versus separation between the two boundaries, $\alpha/\omega_0 = 4$.

---

[1]The expressions for $\mathfrak{f}(\omega_0, \alpha, \frac{L}{2})$ and $\mathfrak{h}(\omega_0, \alpha, z_0, \frac{L}{2})$ are given in Appendix (B).
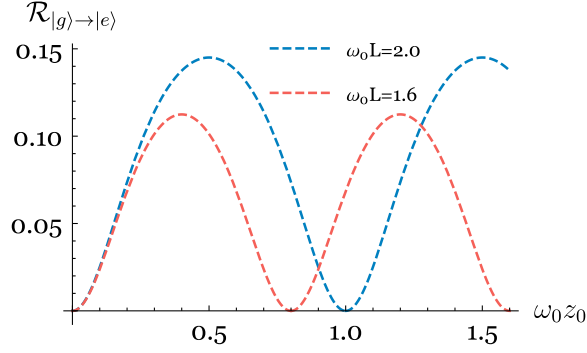[2]The expression for $\mathfrak{g}(\omega_0, \alpha, z_0)$ is given in Appendix (B).

FIG. 3.   Transition rate from $|g\rangle \to |e\rangle$ (per unit $\frac{\lambda^2 \omega_0}{2\pi}$) versus distance of the atom from one boundary, $\alpha/\omega_0 = 4$.

Fig. 2) that with increase in the length of the cavity (L), the rate of upward transition increases.

Figure 4 shows the variation of the transition rate from $|g\rangle \to |e\rangle$ (per unit $\frac{\lambda^2 \omega_0}{2\pi}$) with respect to the acceleration of the atom for different values of the length of the cavity and distance of the atom from one boundary. From the plots, it is observed that for a fixed value of the length of the cavity L and the atomic distance z_0 from one boundary, the
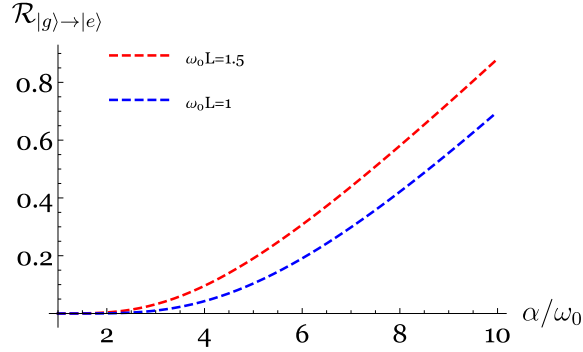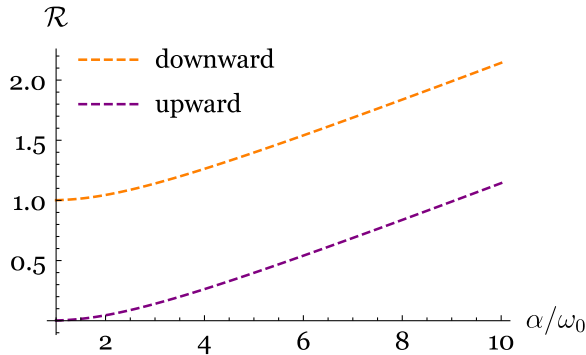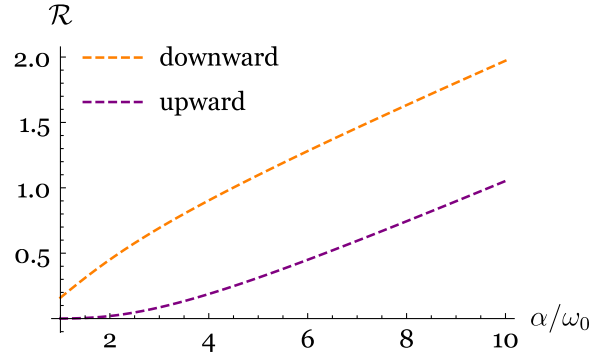

FIG. 4.   Transition rate from $|g\rangle \to |e\rangle$ (per unit $\frac{\lambda^2 \omega_0}{2\pi}$) versus acceleration, $\omega_0 z_0 = 0.3$.

transition rate increases when the acceleration of the atom is increased. Once again we find that the transition rate is more for a larger value of the cavity length which is consistent with our earlier observations.

In Figure 5, we compare the upward and the downward transition rates with respect to the atomic acceleration for two cases, namely, atom in free space (Figure 5a), atom confined to a cavity [Fig. 5(b)]. From the above plots, it is seen that both the transition rates get affected due to the presence of the cavity. As noted earlier, in presence of the cavity the upward and the downward transition rates decrease with decrease in the cavity length. Here it is seen that when $\omega_0 L \sim \omega_0 z_0$, the cavity effect is strong enough to reduce sharply the downward transition rate.

At this point, it might be interesting to make a quantitative estimation of the transition rate for the case when a single atom is placed inside a cavity. Following [74], we choose the length of the cavity in the order of 100 nm, distance between the atom and the nearest boundary in the order of 20 nm, and the acceleration in the order of 10^{17} m/s^2. The energy gap between the ground and excited state of a single Rubidium atom Rb^{87} is of the order of 0.25 eV [91]. Now using Eq. (22) with $\lambda = 0.1$, and the above values, the upward transition rate of the single atom inside a cavity turns out to be 3.38×10^{-12} eV $= 5.12 \times 10^3$ s^{-1}. This tells us that in order to observe a transition to the excited state from the ground state in 1 ns, one would need to perform an experiment with a collection of 10^6 atoms.

IV. TRANSITION RATES OF A SINGLE ATOM FROM THE VIEWPOINT OF A COACCELERATED OBSERVER

In this section, the transitions of a uniformly accelerated atom is analyzed from the perspective of a coaccelerated observer. By definition, a coaccelerated observer moves with an acceleration exactly equal to the acceleration of the

(a) In free space

(b) Inside the cavity for a fixed value of $\omega_0 L = 3$, $\omega_0 z_0 = 0.6$

FIG. 5.   Transition rate (per unit $\frac{\lambda^2 \omega_0}{2\pi}$) versus acceleration.

atom. Therefore, the coaccelerated observer will perceive the atom as being static. Hence, the observer will see no Unruh acceleration radiation as there is no relative acceleration between the observer and the atom. However, for the observer to detect acceleration radiation, the field is assumed to be at an arbitrary temperature T. To calculate the transition rates and see the boundary effects on the transitions of the uniformly accelerated atom, we consider that the coordinates of the coaccelerated frame are the Rindler coordinates (τ, η, y, z) with the following relation with those of the laboratory coordinates (t, x, y, z)

$$t(\tau,\eta) = \frac{1}{\alpha} e^{\alpha\eta} \sinh(\alpha\tau), \quad x(\tau,\eta) = \frac{1}{\alpha} e^{\alpha\eta} \cosh(\alpha\tau). \quad (26)$$

For $\eta = 0$, the above relations reduce to that of the atomic trajectory given in Eq. (10) in the laboratory frame.

In the coaccelerated frame, the field operator $\phi(x(\tau))$ is replaced by its Rindler counterpart $\bar{\phi}(x(\tau))$ [82] and it takes the form [39]

$$\bar{\phi}(\tau, \mathbf{x})) = \int_0^\infty d\omega \int_{-\infty}^\infty dk_y \int_{-\infty}^\infty dk_z$$
$$\times [b_{\omega,k_y,k_z} \mathcal{V}_{\omega,k_y,k_z}(\tau, \mathbf{x}) + b^\dagger_{\omega,k_y,k_z} \mathcal{V}^\star_{\omega,k_y,k_z}(\tau, \mathbf{x})]$$
$$(27)$$

with

$$\mathcal{V}_{\omega,k_y,k_z}(\tau, \mathbf{x}) = \sqrt{\frac{\sinh(\pi\omega/\alpha)}{4\pi^4\alpha}} \mathcal{K}_{i\frac{\omega}{\alpha}}\left(\frac{k_\perp}{\alpha} e^{\alpha\eta}\right) e^{-i\omega\tau + ik_y y + ik_z z}$$
$$(28)$$

being the positive frequency orthonormal mode solution, $\mathcal{K}_\nu(x)$ is the Bessel function of imaginary argument and $k_\perp \equiv |\mathbf{k}_\perp| = \sqrt{k_y^2 + k_z^2}$. The interaction between the atom and the scalar field in this case can be written as [82]

$$H = \lambda m(\tau) \bar{\phi}(x(\tau)). \quad (29)$$

As mentioned earlier, in order to determine the transition rate in the coaccelerated frame, we consider that the field is at an arbitrary temperature T. As the thermal state is a mixed state, therefore to calculate the response of a single atom coupled to the massless scalar field, it is further assumed that the field state can be represented by a pure state $|\sigma_{\omega,k_y,k_z}\rangle$ with a probability factor $p_\sigma(\omega) = e^{-\beta\omega\sigma}/N(\omega)$ with $\beta = 1/T$ and $N(\omega) = \sum_{\sigma=0}^\infty e^{-\beta\omega\sigma}$. In this case, $|\psi_\pm, \sigma_{\omega,k_y,k_z}\rangle$ and $|E_n, \gamma_{\omega',k_y',k_z'}\rangle$ can be used to represent respectively, the initial and the final state of the atom-field system.

Now, following the procedure described in the previous section, the transition probability of the atom-field system from the initial state $|i\rangle$ to final state $|f\rangle$ is given by

$$\mathcal{P}^\beta_{|i\rangle \to |f\rangle} = \lambda^2 |m_{fi}|^2 F^\beta(\Delta E), \quad (30)$$

where the response function $F^\beta(\Delta E)$ is defined as

$$F^\beta(\Delta E) = \int_{-\infty}^{+\infty} d\tau \int_{-\infty}^{+\infty} d\tau' e^{-i\Delta E(\tau-\tau')} G^+_\beta(x(\tau), x(\tau')) \quad (31)$$

and

$$G^+_\beta(x(\tau), x(\tau'))$$
$$= \frac{\text{tr}[\rho' \phi(x(\tau))\phi(x(\tau')]}{\text{tr}[\rho']}$$
$$= N^{-1}(\omega) \sum_{\sigma=0}^\infty \int_0^\infty d\omega \int_{-\infty}^\infty dk_y \int_{-\infty}^\infty dk_z e^{-\beta\omega\sigma}$$
$$\times \langle \sigma_{\omega,k_y,k_z} | \bar{\phi}(x(\tau)) \bar{\phi}(x(\tau')) | \sigma_{\omega,k_y,k_z} \rangle \quad (32)$$

is the positive frequency Wightman function of the scalar field in a thermal state at an arbitrary temperature T in the coaccelerated frame. Exploiting the time translational invariance property of the positive frequency Wightman function, the response function per unit proper time can be written as

$$\mathcal{F}^\beta(\Delta E) = \int_{-\infty}^{+\infty} d(\Delta\tau) e^{-i\Delta E \Delta\tau} G^+_\beta(x(\tau), x(\tau')). \quad (33)$$

Therefore, the transition probability per unit proper time of the atom from the initial state $|i\rangle$ to the final state $|f\rangle$ turns out to be

$$\mathcal{R}^\beta_{|i\rangle \to |f\rangle} = \lambda^2 |m_{fi}|^2 \mathcal{F}^\beta(\Delta E). \quad (34)$$

A. Transition rates in empty space with respect to a coaccelerated observer

In the coaccelerated frame, the trajectory of the atom can be described by

$$t = \tau, \qquad \eta = y = z = 0. \quad (35)$$

Now following the procedure in Appendix C, for an arbitrary temperature T, the thermal Wightman function takes the form

$$G^+_\beta(x(\tau), x(\tau')) = -\frac{1}{4\pi^2} \sum_{s=-\infty}^\infty \frac{1}{(\Delta\tau - is\beta - i\varepsilon)^2}. \quad (36)$$

Using the above Wightman function in Eqs. (33) and (34), the upward and downward transition rates of a single atom submerged in the thermal bath turn out to be

$$\mathcal{R}^{\beta}_{|g\rangle \to |e\rangle} = \frac{\lambda^2 \omega_0}{2\pi} \left(\frac{1}{\exp(\omega_0/T) - 1} \right) \quad (37)$$

$$\mathcal{R}^{\beta}_{|e\rangle \to |g\rangle} = \frac{\lambda^2 \omega_0}{2\pi} \left(1 + \frac{1}{\exp(\omega_0/T) - 1} \right). \quad (38)$$

The above equations suggest that in the coaccelerated frame both the upward and the downward transition can occur for an atom immersed in the thermal bath which is very similar to the transitions observed by an instantaneous inertial observer. Taking the limit $T \to 0$, we can see that the upward transition rate vanishes and this is consistent with the fact that there should be no transition if the observer is static with respect to the atom. Eqs. (16), (17), (37) and (38) clearly indicate that the transition rates of an uniformly accelerated atom seen by an instantaneously inertial observer and by a coaccelerated observer are identical only when if we take the thermal bath temperature in the coaccelerated frame to be $T = \alpha/2\pi$.

B. Transition rates in a cavity from the viewpoint of a coaccelerated observer

In this subsection, we consider a uniformly accelerated atom interacting with a vacuum massless scalar field confined to a cavity of length L from the perspective of a coaccelerated observer. We assume that perfectly reflecting boundaries are placed at $z = 0$ and $z = L$. In a coaccelerated frame, this scenario will be depicted as a static atom interacting with a massless scalar field in a thermal state at an arbitrary temperature T inside a cavity of length L.

In the coaccelerated frame, the trajectory of the atom inside the cavity becomes

$$t = \tau, \qquad \eta = y = 0, \qquad z = z_0. \quad (39)$$

Now following the procedure in Appendix D, for an arbitrary temperature T, the thermal Wightman function inside the cavity takes the form[3]

$$G^+_\beta(x(\tau), x(\tau'))$$
$$= -\frac{1}{4\pi^2} \sum_{n=-\infty}^{\infty} \sum_{s=-\infty}^{\infty} \left[\frac{\mathcal{B}_1}{\mathcal{C}_1} \frac{1}{(\Delta\tau - is\beta - i\varepsilon)^2 - \mathcal{B}_1^2} \right.$$
$$\left. - \frac{\mathcal{B}_2}{\mathcal{C}_2} \frac{1}{(\Delta\tau - is\beta - i\varepsilon)^2 - \mathcal{B}_2^2} \right]. \quad (40)$$

Using above Wightman function in Eqs. (33) and (34), the downward and upward transition rates of the single atom system inside the cavity read

---

[3]The expressions for $\mathcal{B}_1$, $\mathcal{C}_1$, $\mathcal{B}_2$, and $\mathcal{C}_2$ are given in Appendix D.

$$\mathcal{R}^{\beta}_{|g\rangle \to |e\rangle} = \lambda^2 \left[\left\{ \frac{\omega_0}{2\pi} + \mathfrak{f}\left(\omega_0, \alpha, \frac{L}{2}\right) - \mathfrak{h}\left(\omega_0, \alpha, z_0, \frac{L}{2}\right) \right\} \right.$$
$$\left. \times \left(\frac{1}{\exp(\omega_0/T) - 1} \right) \right] \quad (41)$$

$$\mathcal{R}^{\beta}_{|e\rangle \to |g\rangle} = \lambda^2 \left[\left\{ \frac{\omega_0}{2\pi} + \mathfrak{f}\left(\omega_0, \alpha, \frac{L}{2}\right) - \mathfrak{h}\left(\omega_0, \alpha, z_0, \frac{L}{2}\right) \right\} \right.$$
$$\left. \times \left(1 + \frac{1}{\exp(\omega_0/T) - 1} \right) \right]. \quad (42)$$

Next, taking the limit $L \to \infty$, the upward and the downward transition rate in the presence of a single reflecting boundary turn out respectively to be

$$\mathcal{R}^{\beta}_{|g\rangle \to |e\rangle} = \lambda^2 \left[\left\{ \frac{\omega_0}{2\pi} - \mathfrak{g}(\omega_0, \alpha, z_0) \right\} \left(\frac{1}{\exp(\omega_0/T) - 1} \right) \right] \quad (43)$$

$$\mathcal{R}^{\beta}_{|e\rangle \to |g\rangle} = \lambda^2 \left[\left\{ \frac{\omega_0}{2\pi} - \mathfrak{g}(\omega_0, \alpha, z_0) \right\} \left(1 + \frac{1}{\exp(\omega_0/T) - 1} \right) \right] \quad (44)$$

with $\mathfrak{f}(\omega_0, \alpha, \frac{L}{2})$, $\mathfrak{h}(\omega_0, \alpha, z_0, \frac{L}{2})$, and $\mathfrak{g}(\omega_0, \alpha, z_0)$ being the same as in Eqs. (B3)–(B5).

The above analysis clearly displays the similarity between the transitions observed by an instantaneously inertial observer and a coaccelerated observer in a thermal bath for both the upward and the downward transition rates when the atom is confined in a cavity. Here too we notice that taking the thermal bath temperature in the coaccelerated frame $T = \alpha/2\pi$, Eqs. (41), (42), (22) and (23) indicate that the transition rates of a uniformly accelerated atom seen by a coaccelerated observer in a thermal bath and by an instantaneously inertial observer are identical inside the cavity.

V. COUPLING OF THE TWO-ATOM SYSTEM WITH A MASSLESS SCALAR FIELD

We consider two identical atoms A and B and assume that they are traveling along synchronous trajectories in a vacuum with massless scalar field fluctuations, the interatomic distance is assumed to be constant and the proper times of the two atoms can be described by the same time τ [81]. In the laboratory frame, trajectories of the two atoms can be represented through $x_A(\tau)$ and $x_B(\tau)$. Here we consider each atom as a two level system having energy levels $-\omega_0/2$ and $+\omega_0/2$. Therefore, the entire two-atom system can be described by the three energy levels with energies $-\omega_0$, 0 and ω_0 [92]. We designate them by E_n with $n = 1, 2, 3$. The low and high energy levels associated with eigenstates are $|E_1\rangle = |g_A, g_B\rangle$ and $|E_3\rangle = |e_A, e_B\rangle$ where $|g\rangle$ and $|e\rangle$ represent the ground state and the excited

state of a single atom respectively. The energy level E_2 is degenerate corresponding to the eigenstates $|g_A, e_B\rangle$ and $|e_A, g_B\rangle$.

In the instantaneously inertial frame, the Hamiltonian describing the atom-field interaction is given by

$$H = \lambda[m_A(\tau)\phi(x_A(\tau)) + m_B(\tau)\phi(x_B(\tau))], \quad (45)$$

where λ is the atom-field coupling constant assumed to be very small. The forms of $\phi(x(\tau))$ and $m(\tau)$ are the same as given in Eqs. (2) and (3). As a result of the atom-field interaction, transitions also occur for the two-atom system. According to the time-dependent perturbation theory in the first-order approximation, the transition amplitude for the atom-field system to transit from the initial state $|\chi, 0_M\rangle$ to the final state $|\chi', \phi_f\rangle$ is given by

$$\mathcal{A}_{|\chi,0_M\rangle \to |\chi',\phi_f\rangle} = i\lambda\langle\chi', \phi_f| \int_{-\infty}^{+\infty} m_A(\tau)\phi(x_A(\tau))|\chi, 0_M\rangle + A$$
$$\rightleftharpoons B \text{ term.} \quad (46)$$

Squaring the above transition amplitude and summing over all possible field states, the transition probability from the initial state $|\chi\rangle$ to the final state $|\chi'\rangle$ can be written as

$$\mathcal{P}_{|\chi\rangle \to |\chi'\rangle} = \lambda^2[|m_{\chi'\chi}^{(A)}|^2 F_{AA}(\Delta E) + m_{\chi'\chi}^{(B)} m_{\chi'\chi}^{(A)*} F_{AB}(\Delta E)] + A$$
$$\rightleftharpoons B \text{ terms,} \quad (47)$$

where $m_{\chi'\chi}^{(A)} = \langle\chi'|m(0)\otimes\mathbb{1}_B|\chi\rangle$, and $m_{\chi'\chi}^{(B)} = \langle\chi'|\mathbb{1}_A\otimes m(0)|\chi\rangle$. The response function $F_{\xi\xi'}(\Delta E)$ is defined as

$$F_{\xi\xi'}(\Delta E) = \int_{-\infty}^{+\infty} d\tau \int_{-\infty}^{+\infty} d\tau' e^{-i\Delta E(\tau-\tau')}G^+(x_\xi(\tau), x_{\xi'}(\tau'))$$
$$(48)$$

with ξ, ξ' can be labeled by A or B, and

$$G^+(x_\xi(\tau), x_{\xi'}(\tau')) = \langle 0_M|\phi(x_\xi(\tau))\phi(x_{\xi'}(\tau'))|0_M\rangle \quad (49)$$

is the Wightman function of the massless scalar field. From Eq. (47) it is seen that for the two-atom system, the transition probability carries two terms one of them of which is associated with only one of the atoms and other one associated with both the atoms.

Exploiting the time translational invariance property of the Wightman function, the response function per unit proper time can be written as

$$\mathcal{F}_{\xi\xi'}(\Delta E) = \int_{-\infty}^{+\infty} d(\Delta\tau)e^{-i\Delta E\Delta\tau}G^+(x_\xi(\tau), x_{\xi'}(\tau')) \quad (50)$$

where $\Delta\tau = \tau - \tau'$. Therefore, the transition probability per unit proper time of the two-atom system from the initial state $|\chi\rangle$ to the final state $|\chi'\rangle$ turns out to be

$$\mathcal{R}_{|\chi\rangle \to |\chi'\rangle} = \lambda^2[|m_{\chi'\chi}^{(A)}|^2 \mathcal{F}_{AA}(\Delta E) + m_{\chi'\chi}^{(B)} m_{\chi'\chi}^{(A)*} \mathcal{F}_{AB}(\Delta E)] + A$$
$$\rightleftharpoons B \text{ terms.} \quad (51)$$

The existence of the cross terms in the above equation indicates that the rate of transition between the two neighboring energy levels is not only related to the sum of the rates of transition of the two atoms, but also to their cross-correlation.

In the following section, this formalism is used to examine the rate of transitions of a two-atom system under various conditions of uniform acceleration and contact with the vacuum massless scalar field. The correlation between two atoms can be considered as a factor which can affect the transition rate of a two-atom system. In practice, entanglement is not always maintained during experimental conditions, and non-maximally entangled states are frequently used as resources or probes. This motivates us to consider nonmaximally entangled states, as well, in our analysis. The general pure quantum state of the two-atom system is given by [71]

$$|\psi\rangle = \sin\theta|g_A, e_B\rangle + \cos\theta|e_A, g_B\rangle \quad (52)$$

where the entanglement parameter θ lies in the range $0 \leq \theta \leq \pi$. The above quantum state becomes a separable state for the values of $\theta = 0, \pi/2, \pi$ and represents the maximally entangled state for the value $\theta = \pi/4$ (super-radiant state), and $\theta = 3\pi/4$ (subradiant state). Considering the above generic entangled quantum state as the initial state in the following section, we explore how the non-inertial motion of the atoms, nature of the observer, type of the background field and the presence of the boundaries affect the rate of transition of the two-atom system.

VI. TRANSITION RATES OF THE TWO-ATOM SYSTEM FROM THE VIEWPOINT OF A LOCAL INERTIAL OBSERVER

In this part, we analyse the transitions of a uniformly accelerated two-atom system prepared in any generic entangled state $|\psi\rangle$ that interacts with the vacuum massless scalar field from the perspective of a locally inertial observer. To see the boundary effects on the transitions of the uniformly accelerated two-atom system in this scenario, several cases have been studied in the following subsections.

A. Transition rates for entangled atoms in empty space with respect to a local inertial observer

Here we evaluate the transition rates of a two-atom system that is uniformly accelerating while interacting with a vacuum massless scalar field in the absence of any perfectly reflecting boundary. In the laboratory frame, trajectories of both the atoms read

$$t_A(\tau) = t_B(\tau) = \frac{1}{\alpha}\sinh(\alpha\tau), \quad x_A(\tau) = x_B(\tau) = \frac{1}{\alpha}\cosh(\alpha\tau), \quad y_B = y_A + d, \quad z_A = z_B = 0, \tag{53}$$

where d, α, and τ denote the constant interatomic distance, proper acceleration, and the proper time of the two-atom system. Using the scalar field operator Eq. (2) in Eq. (49), the Wightman function becomes [81]

$$G^+(x_\xi(\tau), x_{\xi'}(\tau')) = -\frac{1}{4\pi^2}\frac{1}{(t_\xi(\tau) - t_{\xi'}(\tau') - i\varepsilon)^2 - (x_\xi(\tau) - x_{\xi'}(\tau'))^2 - (y_\xi(\tau) - y_{\xi'}(\tau'))^2 - (z_\xi(\tau) - z_{\xi'}(\tau'))^2}. \tag{54}$$

Substituting Eq. (53) in Eq. (54), the Wightman function turns out to be

$$G^+(x_\xi(\tau), x_{\xi'}(\tau')) = -\frac{\alpha^2}{16\pi^2}\frac{1}{\sinh^2[\frac{1}{2}(\alpha\Delta\tau - i\varepsilon)]} \tag{55}$$

with $\Delta\tau = \tau - \tau'$ for $\xi = \xi'$, and

$$G^+(x_\xi(\tau), x_{\xi'}(\tau')) = -\frac{\alpha^2}{16\pi^2}\frac{1}{\sinh^2[\frac{1}{2}(\alpha\Delta\tau - i\varepsilon)] - \frac{1}{4}d^2\alpha^2} \tag{56}$$

for $\xi \neq \xi'$.

Now following the procedure in Appendix E, we finally obtain the upward and downward transition rates to be

$$\mathcal{R}_{|\psi\rangle\to|e_A e_B\rangle} = \lambda^2\left\{\left(\frac{\omega_0}{2\pi} + \frac{\sin 2\theta \sin(\frac{2\omega_0}{\alpha}\sinh^{-1}(\frac{1}{2}\alpha d))}{2\pi d\sqrt{1 + \frac{1}{4}d^2\alpha^2}}\right)\left(\frac{1}{\exp(2\pi\omega_0/\alpha) - 1}\right)\right\}, \tag{57}$$

and the downward transition rate given by

$$\mathcal{R}_{|\psi\rangle\to|g_A g_B\rangle} = \lambda^2\left\{\left(\frac{\omega_0}{2\pi} + \frac{\sin 2\theta \sin(\frac{2\omega_0}{\alpha}\sinh^{-1}(\frac{1}{2}\alpha d))}{2\pi d\sqrt{1 + \frac{1}{4}d^2\alpha^2}}\right)\left(1 + \frac{1}{\exp(2\pi\omega_0/\alpha) - 1}\right)\right\}. \tag{58}$$

Interestingly, the ratio of the upward and the downward transition rates for the two-atom case is identical with that of the single atom case [Eq. (18)].

B. Transition rates for entangled atoms in a cavity with respect to a local inertial observer

Here we consider that a uniformly accelerated two-atom system interacts with a vacuum massless scalar field confined in a cavity having length L (see Fig. 6).
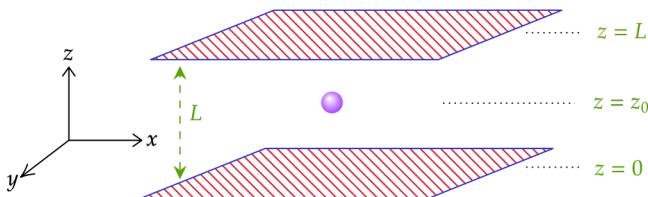
Assuming that the two atoms are moving parallel to the boundary (see Fig. 7) with their proper acceleration similar to the previous case, we investigate the effect of the cavity on the transition rates.

Assuming the scalar field obeys the Dirichlet boundary condition $\phi|_{z=0} = \phi|_{z=L} = 0$, and using the method of images, the Wightman function of the massless scalar field confined to the cavity of length L takes the form

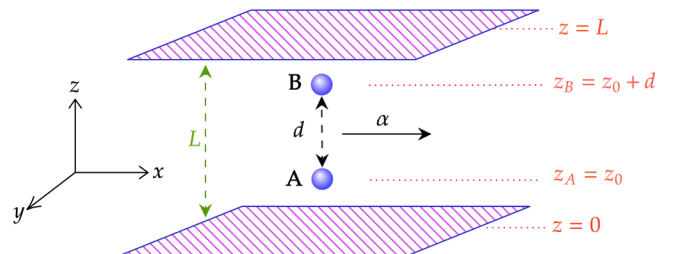FIG. 6.   Static atom confined in a cavity.

FIG. 7.   Uniformly accelerated two-atom confined in a cavity.

$$G^+(x_\xi(\tau), x_{\xi'}(\tau')) = -\frac{1}{4\pi^2} \sum_{n=-\infty}^{\infty} \left[\frac{1}{(t_\xi(\tau) - t_{\xi'}(\tau') - i\varepsilon)^2 - (x_\xi(\tau) - x_{\xi'}(\tau'))^2 - (y_\xi(\tau) - y_{\xi'}(\tau'))^2 - (z_\xi(\tau) - z_{\xi'}(\tau') - nL)^2} \right.$$

$$\left. - \frac{1}{(t_\xi(\tau) - t_{\xi'}(\tau') - i\varepsilon)^2 - (x_\xi(\tau) - x_{\xi'}(\tau'))^2 - (y_\xi(\tau) - y_{\xi'}(\tau'))^2 - (z_\xi(\tau) + z_{\xi'}(\tau') - nL)^2} \right] \tag{59}$$

To represent the atomic trajectories in terms of the atomic proper time τ, we choose the Cartesian coordinates in the laboratory frame so that boundaries are fixed at $z = 0$ and $z = L$.

Considering that the interatomic distance d remains perpendicular while two atoms are moving parallel to the boundary with their proper acceleration, the atomic trajectories are given by

$$t_{A/B}(\tau) = \frac{1}{\alpha}\sinh(\alpha\tau), \qquad x_{A/B}(\tau) = \frac{1}{\alpha}\cosh(\alpha\tau), \qquad y_{A/B} = y_0, \qquad z_A = z_0, \qquad z_B = z_0 + d. \tag{60}$$

Using the above trajectories in Eq. (59), the Wightman function becomes

$$G^+(x_\xi(\tau), x_{\xi'}(\tau')) = -\frac{\alpha^2}{16\pi^2} \sum_{n=-\infty}^{\infty} \left[\frac{1}{\sinh^2[\frac{1}{2}(\alpha\Delta\tau - i\varepsilon)] - \frac{1}{4}d_1^2\alpha^2} - \frac{1}{\sinh^2[\frac{1}{2}(\alpha\Delta\tau - i\varepsilon)] - \frac{1}{4}d_2^2\alpha^2} \right] \tag{61}$$

for $\xi = \xi'$, with $d_1 = nL, d_2 = 2z_\xi - nL$ and

$$G^+(x_\xi(\tau), x_{\xi'}(\tau')) = -\frac{\alpha^2}{16\pi^2} \sum_{n=-\infty}^{\infty} \left[\frac{1}{\sinh^2[\frac{1}{2}(\alpha\Delta\tau - i\varepsilon)] - \frac{1}{4}d_3^2\alpha^2} - \frac{1}{\sinh^2[\frac{1}{2}(\alpha\Delta\tau - i\varepsilon)] - \frac{1}{4}d_4^2\alpha^2} \right] \tag{62}$$

for $\xi \neq \xi'$, with $d_3 = -d - nL$ (for $\xi = A, \xi' = B$); $d_3 = d - nL$ (for $\xi = B, \xi' = A$) and $d_4 = 2z_0 + d - nL$. Now following the procedure in Appendix F, we finally obtain the upward and downward transition rates to be[4]

$$\mathcal{R}_{|\psi\rangle \to |e_A e_B\rangle} = \lambda^2 \left\{ \left(\frac{\omega_0}{2\pi} + \mathfrak{f}\left(\omega_0, \alpha, \frac{L}{2}\right) - \cos^2\theta \mathfrak{h}\left(\omega_0, \alpha, z_0, \frac{L}{2}\right) - \sin^2\theta \mathfrak{m}\left(\omega_0, \alpha, z_0, d, \frac{L}{2}\right) + \sin 2\theta \mathfrak{n}\left(\omega_0, \alpha, \frac{d}{2}, \frac{L}{2}\right) \right. \right.$$

$$\left. \left. - \sin 2\theta \mathfrak{m}\left(\omega_0, \alpha, z_0, \frac{d}{2}, \frac{L}{2}\right) \right) \left(\frac{1}{\exp(2\pi\omega_0/\alpha) - 1} \right) \right\} \tag{63}$$

$$\mathcal{R}_{|\psi\rangle \to |g_A g_B\rangle} = \lambda^2 \left\{ \left(\frac{\omega_0}{2\pi} + \mathfrak{f}\left(\omega_0, \alpha, \frac{L}{2}\right) - \cos^2\theta \mathfrak{h}\left(\omega_0, \alpha, z_0, \frac{L}{2}\right) - \sin^2\theta \mathfrak{m}\left(\omega_0, \alpha, z_0, d, \frac{L}{2}\right) + \sin 2\theta \mathfrak{n}\left(\omega_0, \alpha, \frac{d}{2}, \frac{L}{2}\right) \right. \right.$$

$$\left. \left. - \sin 2\theta \mathfrak{m}\left(\omega_0, \alpha, z_0, \frac{d}{2}, \frac{L}{2}\right) \right) \left(1 + \frac{1}{\exp(2\pi\omega_0/\alpha) - 1} \right) \right\}. \tag{64}$$

In order to obtain the single mirror and free space scenarios, we now take the limiting cases of these expressions. Taking the limit $L \to \infty$, we find that Eqs. (63) and (64) reduce to the expression for the upward and the downward transition rate in the presence of a single reflecting boundary

$$\mathcal{R}_{|\psi\rangle \to |e_A e_B\rangle} = \lambda^2 \left\{ \left(\frac{\omega_0}{2\pi} - \cos^2\theta \mathfrak{g}(\omega_0, \alpha, z_0) - \sin^2\theta \mathfrak{g}(\omega_0, \alpha, (z_0 + d)) \right. \right.$$

$$\left. \left. + \sin 2\theta \left(\mathfrak{g}\left(\omega_0, \alpha, \frac{d}{2}\right) - \mathfrak{g}\left(\omega_0, \alpha, z_0 + \frac{d}{2}\right) \right) \right) \left(\frac{1}{\exp(2\pi\omega_0/\alpha) - 1} \right) \right\} \tag{65}$$

$$\mathcal{R}_{|\psi\rangle \to |g_A g_B\rangle} = \lambda^2 \left\{ \left(\frac{\omega_0}{2\pi} - \cos^2\theta \mathfrak{g}(\omega_0, \alpha, z_0) - \sin^2\theta \mathfrak{g}(\omega_0, \alpha, (z_0 + d)) \right. \right.$$

$$\left. \left. + \sin 2\theta \left(\mathfrak{g}\left(\omega_0, \alpha, \frac{d}{2}\right) - \mathfrak{g}\left(\omega_0, \alpha, z_0 + \frac{d}{2}\right) \right) \right) \left(1 + \frac{1}{\exp(2\pi\omega_0/\alpha) - 1} \right) \right\}. \tag{66}$$

---

[4]The expressions for $\mathfrak{m}(\omega_0, \alpha, z_0, d, \frac{L}{2})$, $\mathfrak{n}(\omega_0, \alpha, z_0, \frac{d}{2}, \frac{L}{2})$ are given in Appendix F.
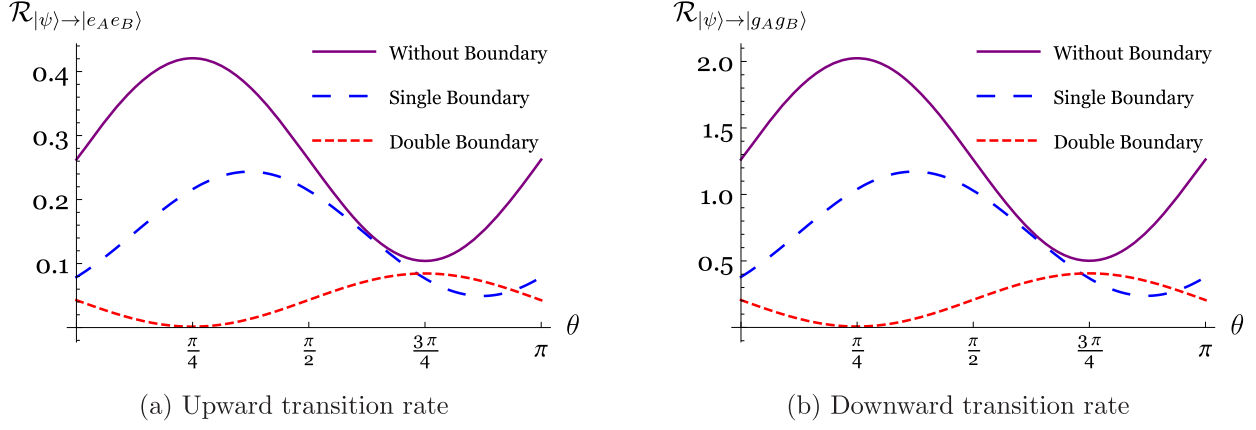
(a) Upward transition rate   (b) Downward transition rate

FIG. 8. Transition rate (per unit $\frac{\lambda^2 \omega_0}{2\pi}$) versus entanglement parameter for a fixed value of $\alpha/\omega_0 = 4, \omega_0 d = 0.5, \omega_0 L = 1, \omega_0 z_0 = 0.2$.

It may be noted that the above relations resemble those of the single boundary results given in [81] but they are not identical as in our case the interatomic distance is perpendicular to the reflecting boundary whereas in [81] the interatomic distance is parallel to the reflecting boundary. Similarly, taking the limits $L \to \infty$ and $z_0 \to \infty$, Eqs. (63) and (64) lead to the expressions for the upward and the downward transition rate in free space given by Eqs. (57) and (58).

We now study the variation of the transition rate of an entangled two atom system from an initial entangled state $|\psi\rangle$ to a product state with higher energy value $|e_A e_B\rangle$ confined to a cavity with the atomic acceleration (α), length of the cavity (L), distance of any one atom from one boundary (z_0), entanglement parameter (θ), and the interatomic distance (d). The findings are plotted below, where all physical quantities are expressed in dimensionless units. Since cavity effects are significant when the length scales are comparable [93], hence we choose a similar order of magnitude for $\omega_0 L, \omega_0 z_0$ and $\omega_0 d$. In Figure 8a, we show the behavior of the transition rate with respect to the entanglement parameter for the cases where the atoms are in free space, in the vicinity of a single boundary and inside a cavity.

From the above figure, it can be seen that the transition rate $|\psi\rangle \to |e_A e_B\rangle$ (per unit $\frac{\lambda^2 \omega_0}{2\pi}$) varies sinusoidally with the entanglement parameter θ. In free space, the transition rate increases (from the case corresponding to the zero entanglement product state) with increase in the entanglement parameter and it becomes maximum when the initial state is maximally entangled ($\theta = \pi/4$ superradiant state). Further increment of the entanglement parameter decreases the transition rate and it becomes minimum at $\theta = 3\pi/4$ (sub-radiant state). In the vicinity of a single boundary, behavior of the transition rate is quite similar to the free space scenario, with a slight shifting of the extremum points). Surprisingly, inside the cavity, the behavior of the transition rate is opposite to the free space scenario. The transition rate decreases with the increase in entanglement

parameter and it vanishes at $\theta = \pi/4$. Thus, the $\theta = \pi/4$ state exhibits a subradiant behavior for the cavity setup. Further increment of entanglement parameter increases the transition rate and it becomes maximum at $\theta = 3\pi/4$. Note also, that around $\theta = 3\pi/4$, the values of the transition rate corresponding to cases of empty space, single boundary, and two boundaries, are nearly the same.

It may be noted however, that the transition rate of the superradiant state ($\theta = \pi/4$) of the two atoms inside the cavity vanishes only for certain specific values of the various parameters we have considered in our study. Increasing the width of the cavity keeping the other parameters fixed, it can be found that the rate of transition does not vanish at $\theta = \pi/4$. Hence, the superradiance property of the state with $\theta = \pi/4$ is lost in such cases. One obtains a superradiant state for a smaller value of the cavity width since in such a scenario, the number of quantum field modes available to the atoms reduces, which makes the atoms unable to perform the transition to any higher/lower energetic separable state.

Figure 8(b) for the downward transition rates shows a similar behavior with respect to the entanglement parameter. The only difference is that the magnitude of the downward transition rate is greater than the upward transition rate. From both the figures, it is observed that when the initial entangled state is the superradiant maximally entangled state ($\theta = \pi/4$), then upward or downward transition rate depends on the width of the cavity. Therefore, this observation indicates that using a small width cavity, for this value of the entanglement parameter, the entanglement of the initial state is preserved.

Figure 9 shows the variation of the transition rate from $|\psi\rangle \to |e_A e_B\rangle$ (per unit $\frac{\lambda^2 \omega_0}{2\pi}$) with respect to the length of the cavity for different values of distance of any one atom from one boundary. From the plots, it can be seen that for a fixed value of the initial atomic distance z_0 of any one atom from the nearest boundary, the transition rate get enhanced when the cavity length increases and attains a maximum value for large values of L ($\omega_0 L \gg \omega_0 z_0$). This behavior is similar to
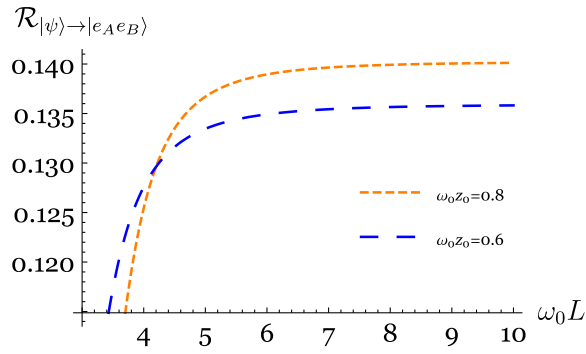
FIG. 9. Transition rate from $|\psi\rangle \to |e_A e_B\rangle$ (per unit $\frac{\lambda^2 \omega_0}{2\pi}$) versus separation between two boundaries, $\alpha/\omega_0 = 4$.

FIG. 11. Transition rate from $|\psi\rangle \to |e_A e_B\rangle$ (per unit $\frac{\lambda^2 \omega_0}{2\pi}$) versus interatomic distance, $\alpha/\omega_0 = 4, \omega_0 L = 1.5$.

that of the single atom case, as mentioned earlier. As more number of field modes take part in the interaction between the scalar field and the atoms due to the increased cavity length, the transition rate increases. When $\omega_0 L \gg \omega_0 z_0$, the cavity scenario reduces to a single boundary set up and hence the upward transition rate takes a constant value. It is also observed that the saturation value of the transition rate is more for a larger value of $\omega_0 z_0$.

Figure 10 shows the variation of the transition rate from $|\psi\rangle \to |e_A e_B\rangle$ (per unit $\frac{\lambda^2 \omega_0}{2\pi}$) with respect to the distance of any one atom from one boundary $\omega_0 z_0$ for different interatomic distances $\omega_0 d$. From the plots, it is observed that for a fixed value of the interatomic distance and cavity length, the transition rate is much smaller when the atoms are close to the any one of the boundaries. Thereafter, with increase of the atomic distance from one boundary, the transition rate rises sharply and reaches maximum when the distance of both atoms to their nearest boundaries are equal. The importance of boundary effects are thereby clearly exhibited. From the plot, it is also seen that increasing the interatomic distance increases the upward transition rate for a fixed cavity length.

Figure 11 shows the variation of the transition rate from $|\psi\rangle \to |e_A e_B\rangle$ (per unit $\frac{\lambda^2 \omega_0}{2\pi}$) with respect to the interatomic

distance for different values of distance of any one atom from one boundary. From the plots, we see that for a fixed atomic distance from one boundary and cavity length, transition rate initially increases when the interatomic distance increases. After a certain value of interatomic distance, increasing the distance between the two atoms further make them move closer to the boundary and hence due to boundary effects, the transition rate falls down.

Figure 12 shows the variation of the transition rate from $|\psi\rangle \to |e_A e_B\rangle$ (per unit $\frac{\lambda^2 \omega_0}{2\pi}$) with respect to the atomic acceleration for different values of cavity length. Similar to the single atom case, it is seen that when the atomic acceleration is increased, the transition rate also increases and the rate of transition depends on the cavity length. This is expected since acceleration radiation should increase with increase in acceleration.

In Fig. 13, we have plotted the upward and the downward transition rates with respect to the atomic acceleration for two cases, namely, two atoms are in free space [Fig. 13(a)], two atoms are confined to a cavity [Figure 13(b)]. A comparison of the two plots reveals that the downward transition rate can get diminished for a suitable choice of parameters when the atoms are inside the cavity. The upward transitions in both cases are driven by the acceleration, as is clear from the corresponding expressions, as well.
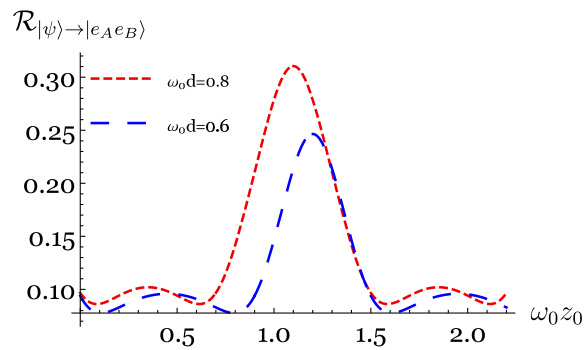

FIG. 10. Transition rate from $|\psi\rangle \to |e_A e_B\rangle$ (per unit $\frac{\lambda^2 \omega_0}{2\pi}$) versus distance of any one atom from one boundary, $\alpha/\omega_0 = 4, \omega_0 L = 3$.
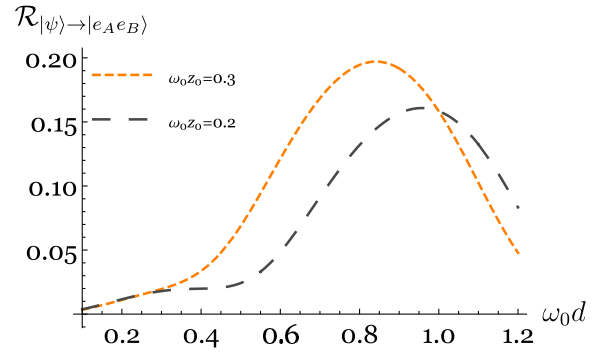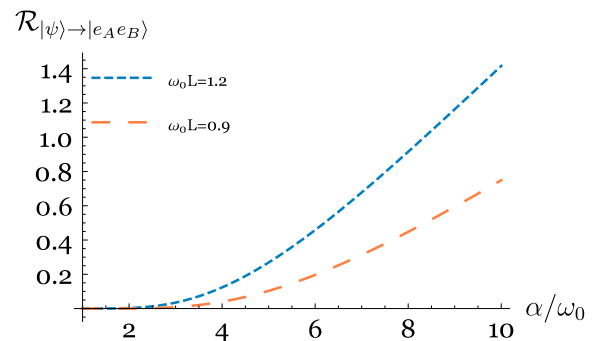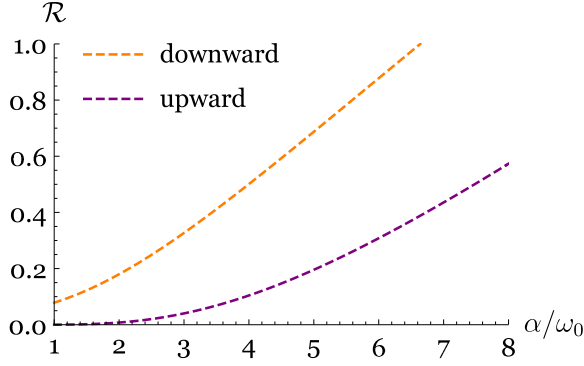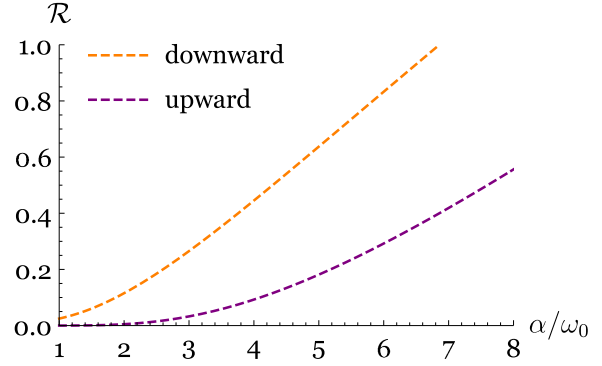

FIG. 12. Transition rate from $|\psi\rangle \to |e_A e_B\rangle$ (per unit $\frac{\lambda^2 \omega_0}{2\pi}$) versus acceleration, $\omega_0 d = 0.5, \omega_0 z_0 = 0.3$.

FIG. 13. Transition rate (per unit $\frac{\lambda^2 \omega_0}{2\pi}$) versus acceleration for a fixed value of $\theta = 3\pi/4, \omega_0 d = 0.5$.

We now present a quantitative estimation of the upward transition rate for the two-atom system, composed of two Rubidium atoms Rb[87] placed inside a cavity. Following [74], we choose the length of the cavity in the order of 100 nm, distance between any one atom and the nearest boundary in the order of 20 nm, interatomic distance in the order of 30 nm, energy gap between the most generic entangled state and excited state of the two-atom system is of the order of 0.5 eV, and the acceleration in the order of 10^{17} m/s^2. Using Eq. (63) with the coupling constant $\lambda = 0.1$, taking the entanglement parameter $\theta = 3\pi/4$ for the maximally entangled state, and the above values, the upward transition rate of the uniformly accelerated two-atom system inside a cavity becomes 3.75×10^{-12} eV $= 5.68 \times 10^3$ s^{-1}.

Before concluding this section, it may be noted that in Ref. [71], the same system was considered. However, the focus there was different from the present study. There, the resonance energy shift and the relaxation rate of energy of the entangled two-atom system were obtained. The present analysis investigates, on the other hand, the transition rate with the aim of studying the equivalence of two different frames.

VII. TRANSITION RATES OF THE TWO-ATOM SYSTEM FROM THE VIEWPOINT OF A COACCELERATED OBSERVER

In this section, the transitions of a uniformly accelerated two-atom system prepared in any generic entangled state $|\psi\rangle$ that interacts with a massless scalar field is analyzed from the perspective of a coaccelerated observer. To see the boundary effects on the transitions of the uniformly accelerated two-atom system in this scenario, we consider that the coordinate of the coaccelerated frame will be the Rindler coordinate (τ, η, y, z) with the relation with those of the laboratory coordinates (t, x, y, z) being given by

$$t(\tau, \eta) = \frac{1}{\alpha} e^{\alpha\eta} \sinh(\alpha\tau), \quad x(\tau, \eta) = \frac{1}{\alpha} e^{\alpha\eta} \cosh(\alpha\tau). \quad (67)$$

In the coaccelerated frame, the field operator $\phi(x(\tau))$ is replaced by its Rindler counterpart $\bar{\phi}(x(\tau))$ and takes the form

$$\bar{\phi}(\tau, \mathbf{x})) = \int_0^\infty d\omega \int_{-\infty}^\infty dk_y \int_{-\infty}^\infty dk_z$$
$$\times [b_{\omega,k_y,k_z} \mathcal{V}_{\omega,k_y,k_z}(\tau, \mathbf{x}) + b^\dagger_{\omega,k_y,k_z} \mathcal{V}^\star_{\omega,k_y,k_z}(\tau, \mathbf{x})]$$

$$(68)$$

with

$$\mathcal{V}_{\omega,k_y,k_z}(\tau, \mathbf{x}) = \sqrt{\frac{\sinh(\pi\omega/\alpha)}{4\pi^4\alpha}} \mathcal{K}_{i\frac{\omega}{\alpha}}\left(\frac{k_\perp}{\alpha} e^{\alpha\eta}\right) e^{-i\omega\tau + ik_y y + ik_z z}$$

$$(69)$$

being the positive frequency orthonormal mode solution, $\mathcal{K}_\nu(x)$ is the Bessel function of imaginary argument and $k_\perp \equiv |\mathbf{k_\perp}| = \sqrt{k_y^2 + k_z^2}$. The interaction between the atoms and the scalar field is given by [82]

$$H = \lambda[m_A(\tau)\bar{\phi}(x_A(\tau)) + m_B(\tau)\bar{\phi}(x_B(\tau))]. \quad (70)$$

To determine the transition rate of the two-atom system in the coaccelerated frame, we consider a thermal field at an arbitrary temperature T. As the thermal state is a mixed state, in order to calculate the response of the two atoms coupled to the massless scalar field, additionally it is assumed that the field state can be represented by a pure state $|\sigma_{\omega,k_y,k_z}\rangle$ with a probability factor $p_\sigma(\omega) = e^{-\beta\omega\sigma}/N(\omega)$ with $\beta = 1/T$ and $N(\omega) = \sum_{\sigma=0}^\infty e^{-\beta\omega\sigma}$. In this case, $|\psi, \sigma_{\omega,k_y,k_z}\rangle$ and $|E_n, \gamma_{\omega',k'_y,k'_z}\rangle$ can be used to represent the initial and the final state of the atom-field system.

Following the procedure described in the previous sections, the probability that the atom-field system will transit from initial state $|\psi\rangle$ to final state $|E_n\rangle$ is then given by

$$\mathcal{P}_{|\psi_\pm\rangle \to |E_n\rangle} = \lambda^2 [|m^{(A)}_{E_n\psi_\pm}|^2 F^\beta_{AA}(\Delta E) + m^{(B)}_{E_n\psi_\pm} m^{(A)*}_{E_n\psi_\pm} F^\beta_{AB}(\Delta E)] + A \rightleftharpoons B \text{ terms.} \tag{71}$$

The response function $F^\beta_{\xi\xi'}(\Delta E)$ is defined as

$$F^\beta_{\xi\xi'}(\Delta E) = \int_{-\infty}^{+\infty} d\tau \int_{-\infty}^{+\infty} d\tau' e^{-i\Delta E(\tau-\tau')} G^+_\beta(x_\xi(\tau), x_{\xi'}(\tau')) \tag{72}$$

with ξ, ξ' labeled by A or B, and

$$G^+_\beta(x_\xi(\tau), x_{\xi'}(\tau')) = \frac{\text{tr}[\rho'\phi(x_\xi(\tau))\phi(x_{\xi'}(\tau'))]}{\text{tr}[\rho']}$$

$$= N^{-1}(\omega) \sum_{\sigma=0}^{\infty} \int_0^\infty d\omega \int_{-\infty}^\infty dk_y \int_{-\infty}^\infty dk_z e^{-\beta\omega\sigma} \langle \sigma_{\omega,k_y,k_z} | \bar\phi(x_\xi(\tau)) \bar\phi(x_{\xi'}(\tau')) | \sigma_{\omega,k_y,k_z} \rangle \tag{73}$$

is the positive frequency Wightman function of the scalar field in a thermal state at an arbitrary temperature T in the coaccelerated frame. Exploiting the time translational invariance property of the Wightman function, the response function per unit proper time can be written as

$$\mathcal{F}^\beta_{\xi\xi'}(\Delta E) = \int_{-\infty}^{+\infty} d(\Delta\tau) e^{-i\Delta E\Delta\tau} G^+_\beta(x_\xi(\tau), x_{\xi'}(\tau')). \tag{74}$$

Therefore, the transition probability per unit proper time of the two-atom system from the initial state $|\chi\rangle$ to the final state $|\chi'\rangle$ turns out to be

$$\mathcal{R}^\beta_{|\chi\rangle \to |\chi'\rangle} = \lambda^2 [|m^{(A)}_{\chi'\chi}|^2 \mathcal{F}^\beta_{AA}(\Delta E) + m^{(B)}_{\chi'\chi} m^{(A)*}_{\chi'\chi} \mathcal{F}^\beta_{AB}(\Delta E)] + A$$

$$\rightleftharpoons B \text{ terms.} \tag{75}$$

A. Transition rates for entangled atoms in empty space with respect to a coaccelerated observer

In the frame of coaccelerated observer, the trajectories of both the atoms are given by

$$t_{A/B} = \tau, \quad \eta_{A/B} = 0, \quad y_{A/B} = 0, \quad z_A = 0 \quad z_B = d. \tag{76}$$

Now following the procedure in Appendix G, for an arbitrary temperature T, the thermal Wightman function takes the form[5] [82]

$$G^+_\beta(x_\xi(\tau), x_{\xi'}(\tau')) = -\frac{1}{4\pi^2} \sum_{s=-\infty}^{\infty} \frac{1}{(\Delta\tau - is\beta - i\varepsilon)^2} \tag{77}$$

for $\xi = \xi'$, and

---

[5]The expressions for $\mathcal{B}, \mathcal{C}$ are given in Appendix G.

$$G^+_\beta(x_\xi(\tau), x_{\xi'}(\tau')) = -\frac{\mathcal{B}}{4\pi^2\mathcal{C}} \sum_{s=-\infty}^{\infty} \frac{1}{(\Delta\tau - is\beta - i\varepsilon)^2 - \mathcal{B}^2} \tag{78}$$

for $\xi \neq \xi'$.

Using above Wightman functions into Eqs. (74) and (75), and performing the integrations using contour integration, the upward and downward transition rates of the two-atom system submerged in the thermal bath turn out to be

$$\mathcal{R}^\beta_{|\psi\rangle \to |e_A e_B\rangle} = \lambda^2 \left\{ \left(\frac{\omega_0}{2\pi} + \frac{\sin 2\theta \sin(\frac{2\omega_0}{\alpha} \sinh^{-1}(\frac{1}{2}\alpha d))}{2\pi d \sqrt{1 + \frac{1}{4}d^2\alpha^2}} \right) \right.$$

$$\left. \times \left(\frac{1}{\exp(\omega_0/T) - 1} \right) \right\} \tag{79}$$

$$\mathcal{R}^\beta_{|\psi\rangle \to |g_A g_B\rangle} = \lambda^2 \left\{ \left(\frac{\omega_0}{2\pi} + \frac{\sin 2\theta \sin(\frac{2\omega_0}{\alpha} \sinh^{-1}(\frac{1}{2}\alpha d))}{2\pi d \sqrt{1 + \frac{1}{4}d^2\alpha^2}} \right) \right.$$

$$\left. \times \left(1 + \frac{1}{\exp(\omega_0/T) - 1} \right) \right\}. \tag{80}$$

From the above equations it follows that in the coaccelerated frame both the upward and the downward transitions can occur for the two-atom system immersed in the thermal bath which is very similar to the transitions observed by an instantaneously inertial observer. Taking the limiting value of the temperature of the coaccelerated frame $T \to 0$, here also we can see that the upward transition rate vanishes, which is consistent with that in the Minkowski vacuum [Eq. (57)]. Eqs. (57), (58), (79) and (80) indicate that the transition rates of the uniformly accelerated two-atom system in the generic entangled state seen by an instantaneously inertial observer and by a coaccelerated observer are identical only if the thermal bath temperature in the coaccelerated frame is equal to the FDU temperature $T = \alpha/2\pi$.

B. Transition rates for entangled atoms in a cavity with respect to a coaccelerated observer

Here we consider that a uniformly accelerated two-atom system interacts with a massless scalar field confined to a cavity of length L from the perspective of a coaccelerated observer. We assume that two p erfectly reflecting boundaries are placed at $z = 0$ and $z = L$ (see Fig. 14). As in the case of the single atom, the scenario here too depicts a static two-atom system interacting with a massless scalar field in a thermal state at an arbitrary temperature T inside a cavity of length L.

Considering the inter-atomic distance d to remain perpendicular while the two atoms are moving parallel to the boundaries with their proper acceleration, the atomic trajectories are given by
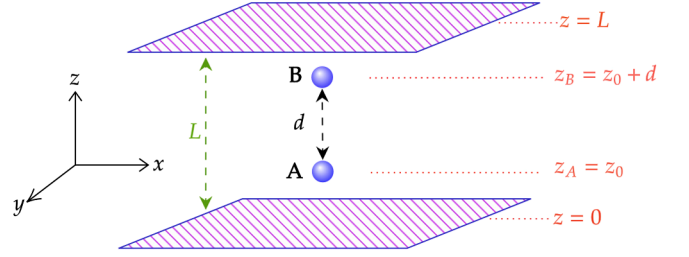

FIG. 14.   Static two-atom confined in a cavity.

$$t_{A/B} = \tau, \qquad \eta_{A/B} = 0,$$
$$y_{A/B} = 0, \qquad z_A = z_0 \quad z_B = z_0 + d. \tag{81}$$

Now following the procedure in Appendix H, for an arbitrary temperature T, the thermal Wightman function takes the form[6]

$$G_\beta^+(x_\xi(\tau), x_{\xi'}(\tau')) = -\frac{1}{4\pi^2} \sum_{n=-\infty}^{\infty} \sum_{s=-\infty}^{\infty} \left[\frac{\mathcal{B}_1}{\mathcal{C}_1} \frac{1}{(\Delta\tau - is\beta - i\varepsilon)^2 - \mathcal{B}_1^2} - \frac{\mathcal{B}_3}{\mathcal{C}_3} \frac{1}{(\Delta\tau - is\beta - i\varepsilon)^2 - \mathcal{B}_3^2} \right] \tag{82}$$

for $\xi = \xi'$ and

$$G_\beta^+(x_\xi(\tau), x_{\xi'}(\tau')) = -\frac{1}{4\pi^2} \sum_{n=-\infty}^{\infty} \sum_{s=-\infty}^{\infty} \left[\frac{\mathcal{B}_4}{\mathcal{C}_4} \frac{1}{(\Delta\tau - is\beta - i\varepsilon)^2 - \mathcal{B}_4^2} - \frac{\mathcal{B}_5}{\mathcal{C}_5} \frac{1}{(\Delta\tau - is\beta - i\varepsilon)^2 - \mathcal{B}_5^2} \right] \tag{83}$$

for $\xi \neq \xi'$.

Inserting the above Wightman functions into Eqs. (74) and (75), and performing the integrations using the contour integration technique, the upward and downward transition rates of the two-atom system submerged in the thermal bath read

$$\mathcal{R}_{|\psi\rangle \to |e_A e_B\rangle}^\beta = \lambda^2 \left\{ \left(\frac{\omega_0}{2\pi} + \mathfrak{f}\left(\omega_0, \alpha, \frac{L}{2}\right) - \cos^2\theta \mathfrak{h}\left(\omega_0, \alpha, z_0, \frac{L}{2}\right) - \sin^2\theta \mathfrak{m}\left(\omega_0, \alpha, z_0, d, \frac{L}{2}\right) + \sin 2\theta \mathfrak{n}\left(\omega_0, \alpha, \frac{d}{2}, \frac{L}{2}\right) \right. \right.$$
$$\left. \left. - \sin 2\theta \mathfrak{m}\left(\omega_0, \alpha, z_0, \frac{d}{2}, \frac{L}{2}\right) \right) \left(\frac{1}{\exp(\omega_0/T) - 1} \right) \right\} \tag{84}$$

$$\mathcal{R}_{|\psi\rangle \to |g_A g_B\rangle}^\beta = \lambda^2 \left\{ \left(\frac{\omega_0}{2\pi} + \mathfrak{f}\left(\omega_0, \alpha, \frac{L}{2}\right) - \cos^2\theta \mathfrak{h}\left(\omega_0, \alpha, z_0, \frac{L}{2}\right) - \sin^2\theta \mathfrak{m}\left(\omega_0, \alpha, z_0, d, \frac{L}{2}\right) + \sin 2\theta \mathfrak{n}\left(\omega_0, \alpha, \frac{d}{2}, \frac{L}{2}\right) \right. \right.$$
$$\left. \left. - \sin 2\theta \mathfrak{m}\left(\omega_0, \alpha, z_0, \frac{d}{2}, \frac{L}{2}\right) \right) \left(1 + \frac{1}{\exp(\omega_0/T) - 1} \right) \right\} \tag{85}$$

where the functions $\mathfrak{f}(\omega_0, \alpha, \frac{L}{2})$, $\mathfrak{h}(\omega_0, \alpha, z_0, \frac{L}{2})$, and $\mathfrak{g}(\omega_0, \alpha, z_0)$ are defined in Appendix B. The functions $\mathfrak{m}(\omega_0, \alpha, z_0, d, \frac{L}{2})$ and $\mathfrak{n}(\omega_0, \alpha, \frac{d}{2}, \frac{L}{2})$ are defined in Appendix F.

By taking the limiting cases of the expressions Eqs. (84) and (85), one can obtain the results of single mirror and free space scenarios. Taking the limit $L \to \infty$, Eqs. (84) and (85) reduce to the expression for the upward and the downward transition rates in the presence of a single reflecting boundary, respectively given by

$$\mathcal{R}_{|\psi\rangle \to |e_A e_B\rangle}^\beta = \lambda^2 \left\{ \left(\frac{\omega_0}{2\pi} - \cos^2\theta \mathfrak{g}(\omega_0, \alpha, z_0) - \sin^2\theta \mathfrak{g}(\omega_0, \alpha, (z_0 + d)) \right. \right.$$
$$\left. \left. + \sin 2\theta \left(\mathfrak{g}\left(\omega_0, \alpha, \frac{d}{2}\right) - \mathfrak{g}\left(\omega_0, \alpha, z_0 + \frac{d}{2}\right) \right) \right) \left(\frac{1}{\exp(\omega_0/T) - 1} \right) \right\} \tag{86}$$

---

[6]The expressions for $\mathcal{B}_1$, $\mathcal{C}_1$ are given in Appendix D and the expressions for $\mathcal{B}_3$, $\mathcal{C}_3$, $\mathcal{B}_4$, $\mathcal{C}_4$, $\mathcal{B}_5$, and $\mathcal{C}_5$ are given in Appendix H.

$$\mathcal{R}^{\beta}_{|\psi\rangle \to |g_A g_B\rangle} = \lambda^2 \Bigg\{ \left(\frac{\omega_0}{2\pi} - \cos^2\theta \mathfrak{g}(\omega_0, \alpha, z_0) - \sin^2\theta \mathfrak{g}(\omega_0, \alpha, (z_0 + d)) \right.$$

$$\left. + \sin 2\theta \left(\mathfrak{g}\left(\omega_0, \alpha, \frac{d}{2}\right) - \mathfrak{g}\left(\omega_0, \alpha, z_0 + \frac{d}{2}\right) \right) \right) \left(1 + \frac{1}{\exp(\omega_0/T) - 1} \right) \Bigg\}. \tag{87}$$

On the other hand, taking the limits $L \to \infty$ and $z_0 \to \infty$ simultaneously, Eqs. (84) and (85) lead to the expression for the upward and the downward transition rates in free space given by Eqs. (79) and (80).

From the above analysis of the two-atom system confined to a cavity, we find a similarity between an instantaneously inertial observer and a coaccelerated observer in a thermal bath for both the upward and the downward transition rates. Here too it may be noted that upon taking the thermal bath temperature in the coaccelerated frame $T = \alpha/2\pi$, from Eqs. (84), (85), (63) and (64) it follows that the transition rates of the uniformly accelerated two-atom system in the generic entangled state seen by a coaccelerated observer and by an instantaneously inertial observer are identical inside the cavity.

VIII. CONCLUSIONS

In this study, we have investigated the transition rates of uniformly accelerated single and entangled two-atom systems. The two-atom system is assumed to be prepared in the most generic pure entangled state. Both systems interact with the massless scalar field from the perspective of an instantaneously inertial observer and a coaccelerated observer, respectively. We have studied the interaction between the accelerated atomic systems and the massless scalar field in two scenarios, namely, free space and inside a cavity. We have presented two examples of the computation of the actual values of the transition rates using realistic system and cavity parameters.

Considering that the scalar field with which the atoms interact in the inertial frame and the coaccelerated frame, are in the vacuum state and a thermal state, respectively, it is seen that in all the above cases, both the upward and the downward transitions take place for the single as well as the entangled two-atom system. The upward transition is nontrivial, and from the view point of an inertial observer, takes place only due to the acceleration of the atomic systems. Our study shows we that the transition rate depends on the cavity parameters, such as the length of the cavity (L), distance of an atom from one boundary (z_0), as well as other system parameters, such as the atomic acceleration (α), the interatomic distance (d), and the magnitude of initial atomic entanglement (θ).

From the analysis, it is observed that for a single atom, the upward transition rate increases with the increment of atomic acceleration and cavity length. The transition rate exhibits an oscillatory behavior with respect to the distance

between the atom and the reflecting boundary. In case of the two-atom system, the transition rates shows some interesting features. In this scenario, the entanglement parameter and the interatomic distance play important roles. The transition rate shows oscillatory behavior in the full range of the entanglement parameter. However, considering a small magnitude of initial entanglement, we find that in the free space, increasing the entanglement parameter enhances the upward transition and downward transition rates, whereas, in the presence of cavity it shows a completely opposite behavior, and both transition rates get suppressed due to the increase of the entanglement parameter. In the case when the entanglement parameter has the value $\theta = \pi/4$, we observe that both the transition rates vanish, indicating that no transition there occurs from the maximally entangled initial state to any higher or lower energetic product state. Hence, the entanglement of the initial state can be preserved. From a quantum information theoretic viewpoint, this result is of significance, since preservation of entanglement enables its use as resource for performing various tasks.

Our study further reveals that the upward transition rate diminishes beyond a certain level of increase of the interatomic distance. From a physical perspective, one may view this result to originate from the fact that the cooperative effects of the two atoms mediated by the field become more and more subdued as the interatomic distance increases beyond a point. On the other hand, the effect due to the distance of an atom from the boundary has a more subtle manifestation. We find that the upward transition rate increases when we increase the distance between any one of the atoms and one boundary, and takes the maximum value when the distance between both atoms to their closest boundaries are equal. Apart from this, the behavior of the transition rate with respect to atomic acceleration and the cavity length is quite similar to the single atom case.

From our extensive study of the transition rates of the single and two-atom systems in an inertial and a coaccelerated frame, we observe that if the temperature of the thermal bath in the coaccelerated frame is taken to be the same as the Unruh temperature, then the transition rates for the upward and the downward transitions in the two frames coincide exactly with each other even inside the cavity, making it completely consistent with the Fulling-Davies-Unruh effect. Therefore, from the present study, the equivalence between the effect of uniform acceleration and the effect of thermal bath is clearly manifested for the

single as well as the entangled two-atom cases in free space and in the presence of reflecting boundaries, as well. The finding is intriguing for the cavity case since the physics changes quite a bit inside a cavity, and moreover such a set-up is experimentally implementable [56,57,83,84].

ACKNOWLEDGMENTS

APPENDIX A: CALCULATIONAL DETAILS OF SOME USEFUL INTEGRALS USED IN THE TEXT

In this Appendix, for the sake of completeness, we provide a detailed calculation of the following integrals

$$\mathcal{I}_1 = -\frac{\alpha^2}{16\pi^2} \int_{-\infty}^{+\infty} d(\Delta\tau) e^{-i\Delta E\Delta\tau} \frac{1}{\sinh^2[\frac{1}{2}(\alpha\Delta\tau - i\epsilon)]} \quad (A1)$$

$$\mathcal{I}_2 = -\frac{\alpha^2}{16\pi^2} \int_{-\infty}^{+\infty} d(\Delta\tau) e^{-i\Delta E\Delta\tau} \frac{1}{\sinh^2[\frac{1}{2}(\alpha\Delta\tau - i\epsilon)] - d^2\alpha^2}. \quad (A2)$$

To solve the integral given in Eq. (A1), we first consider some dimensionless parameters such as $\alpha\Delta\tau = \sigma$, $\Delta E/\alpha = \xi$, and use the series representation [94]

$$\text{csch}^2\left[\frac{1}{2}(\sigma - i\epsilon)\right] = \sum_{k=-\infty}^{\infty} \frac{4}{(\sigma - i\epsilon - 2i\pi k)^2}. \quad (A3)$$

Equation (A1) now becomes

$$\mathcal{I}_1 = -\frac{\alpha}{4\pi^2} \sum_{k=-\infty}^{\infty} \int_{-\infty}^{+\infty} d\sigma \frac{e^{-i\xi\sigma}}{(\sigma - i\epsilon - 2i\pi k)^2}$$

$$= -\frac{\alpha}{4\pi^2} \left[\mathcal{I}_0 + \sum_{k=1}^{\infty} \mathcal{I}_k\right] \quad (A4)$$

where $\mathcal{I}_0$ and $\mathcal{I}_k$ are given by the integrals

$$\mathcal{I}_0 = \int_{-\infty}^{+\infty} d\sigma \frac{e^{-i\xi\sigma}}{(\sigma - i\epsilon)^2} \quad (A5)$$

$$\mathcal{I}_k = \int_{-\infty}^{+\infty} d\sigma e^{-i\xi\sigma} \left\{\frac{1}{(\sigma - 2i\pi k)^2} + \frac{1}{(\sigma + 2i\pi k)^2}\right\}. \quad (A6)$$

Considering the analytic continuation of the above integrands in the complex plane of σ, for Eq. (A5) we get a second order pole at $\sigma = i\epsilon$ and for Eq. (A6) we find a set of second order poles at $\sigma = -2i\pi k$ with

$k = \pm 1, \pm 2, \ldots$, lying on the imaginary axis of σ. For $\xi < 0$ or $\Delta E < 0$, we close the contour in the upper half complex plane in Fig. 15. Using Jordon's lemma, we observe that the integration along the half circle is zero. Therefore, applying the Cauchy residue theorem in the integrals (A5) and (A6) and using it in Eq. (A4), we get

$$\mathcal{I}_1(\Delta E < 0) = -\frac{\alpha}{4\pi^2}\left[2\pi\xi + 2\pi\xi \sum_{k=1}^{\infty} e^{2\pi k\xi}\right]$$

$$= \frac{\alpha|\xi|}{2\pi}\left[1 + \frac{1}{e^{2\pi|\xi|} - 1}\right]$$

$$= \frac{|\Delta E|}{2\pi}\left[1 + \frac{1}{e^{2\pi|\Delta E|/\alpha} - 1}\right]. \quad (A7)$$

Similarly, for $\Delta E > 0$, closing the contour in the lower half complex plane and following the previous steps, we get

$$\mathcal{I}_1(\Delta E > 0) = \frac{\Delta E}{2\pi}\frac{1}{e^{2\pi\Delta E/\alpha} - 1}. \quad (A8)$$

Therefore, combining the above results (A7) and (A8), we get

$$\mathcal{I}_1 = \theta(-\Delta E)\frac{|\Delta E|}{2\pi}\left(1 + \frac{1}{\exp(2\pi|\Delta E|/\alpha) - 1}\right)$$

$$+ \theta(\Delta E)\frac{\Delta E}{2\pi}\left(\frac{1}{\exp(2\pi\Delta E/\alpha) - 1}\right) \quad (A9)$$

where $\theta(\Delta E)$ is defined in Eq. (15).

To evaluate the integral in Eq. (A2), first we consider the analytic continuation of the integrand in the complex plane σ. Equation (A2) then becomes

$$\mathcal{I}_2 = -\frac{\alpha}{16\pi^2}\oint_C d\sigma e^{-i\xi\sigma}\frac{1}{\sinh^2[\frac{1}{2}(\sigma - i\epsilon)] - d^2\alpha^2} \quad (A10)$$

where C is the contour in Fig. 16. From the integrand we find that there exists two types of first order poles $\sigma^+ = i\epsilon + 2in\pi + 2\sinh^{-1}(d\alpha)$ and $\sigma^- = i\epsilon + 2in\pi - 2\sinh^{-1}(d\alpha)$ where $n = 0, \pm 1, \pm 2, \ldots$, lying in the upper and lower half
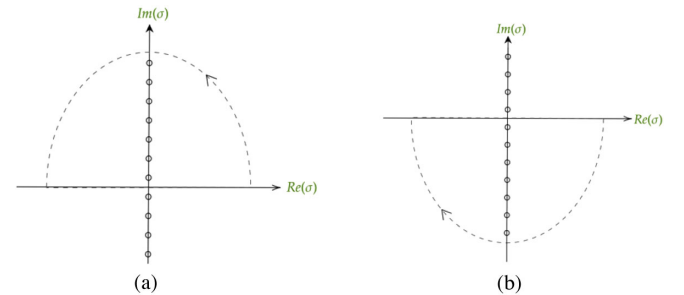

FIG. 15. The contour of the integral Eq. (A1) for (a) $\Delta E < 0$ and (b) $\Delta E > 0$.
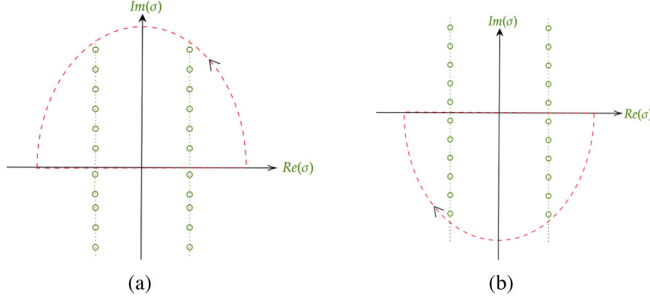
FIG. 16.   The contour of the integral (A2) for (a) $\Delta E < 0$ and (b) $\Delta E > 0$.

of the complex plane. Therefore, closing the contour in the upper half complex plane for $\Delta E < 0$, we find that both the poles will contribute for all positive integer values of n including $n = 0$.

Now applying the residue theorem and taking the limit $\varepsilon \to 0$, the residues become

$$R_1(n) = \frac{\exp -i\frac{\Delta E}{\alpha}(2in\pi + 2\sinh^{-1}(d\alpha))}{\alpha d\sqrt{1+d^2\alpha^2}} \qquad (A11)$$

and

$$R_2(n) = -\frac{\exp -i\frac{\Delta E}{\alpha}(2in\pi - 2\sinh^{-1}(d\alpha))}{\alpha d\sqrt{1+d^2\alpha^2}}. \qquad (A12)$$

Applying Jordon's lemma, we already observe that the integration along the half circle is zero, therefore we get

$$\mathcal{I}_2(\Delta E < 0) = -\frac{\alpha}{16\pi^2}\sum_{n=0}^{\infty} 2\pi i[R_1(n) + R_2(n)]$$

$$= \frac{\sin\left(\frac{2|\Delta E|}{\alpha}\sinh^{-1}(d\alpha)\right)}{4\pi d\sqrt{1+d^2\alpha^2}}\left(1+\frac{1}{e^{2\pi|\Delta E|/\alpha}-1}\right).$$

$$(A13)$$

Similarly, for $\Delta E > 0$, closing the contour in the lower half complex plane we find that both the poles will contribute for all negative integer values of n.

Now following the steps of the case $\Delta E < 0$, we get

$$\mathcal{I}_2(\Delta E > 0) = \frac{\sin\left(\frac{2\Delta E}{\alpha}\sinh^{-1}(d\alpha)\right)}{4\pi d\sqrt{1+d^2\alpha^2}}\left(\frac{1}{e^{2\pi\Delta E/\alpha}-1}\right). \quad (A14)$$

Therefore, combining the above results (A13) and (A14), we get

$$\mathcal{I}_2 = \theta(-\Delta E)\frac{\sin\left(\frac{2|\Delta E|}{\alpha}\sinh^{-1}(d\alpha)\right)}{4\pi d\sqrt{1+d^2\alpha^2}}\left(1+\frac{1}{e^{2\pi|\Delta E|/\alpha}-1}\right)$$

$$+ \theta(\Delta E)\frac{\sin\left(\frac{2\Delta E}{\alpha}\sinh^{-1}(d\alpha)\right)}{4\pi d\sqrt{1+d^2\alpha^2}}\left(\frac{1}{e^{2\pi\Delta E/\alpha}-1}\right). \quad (A15)$$

APPENDIX B: TRANSITION RATES OF A SINGLE ATOM IN A CAVITY WITH RESPECT TO A LOCAL INERTIAL OBSERVER

In this Appendix, we present some of the intermediate steps leading to Eqs. (22) and (23). The form of the Wightman function for the trajectory of an atom inside a cavity is given in Eq. (21). Substituting this form in Eq. (8), the transition rate from the initial state $|i\rangle$ to the final state $|f\rangle$ is given by

$$\mathcal{R}_{|i\rangle\to|f\rangle} = -\frac{\lambda^2|m_{fi}|^2\alpha^2}{16\pi^2}\sum_{n=-\infty}^{\infty}\left[\int_{-\infty}^{+\infty}d(\Delta\tau)e^{-i\Delta E\Delta\tau}\frac{1}{\sinh^2[\frac{1}{2}(\alpha\Delta\tau-i\varepsilon)]-\frac{1}{4}d_1^2\alpha^2}\right.$$

$$\left. -\int_{-\infty}^{+\infty}d(\Delta\tau)e^{-i\Delta E\Delta\tau}\frac{1}{\sinh^2[\frac{1}{2}(\alpha\Delta\tau-i\varepsilon)]-\frac{1}{4}d_2^2\alpha^2}\right]. \qquad (B1)$$

Simplifying the above equation through a contour integral as shown in Appendix A, the rate of transition from the initial state $|i\rangle$ to the final state $|f\rangle$ can be written as

$$\mathcal{R}_{|i\rangle\to|f\rangle} = \lambda^2|m_{fi}|^2\left[\theta(-\Delta E)\left\{\frac{|\Delta E|}{2\pi}+\mathfrak{f}\left(|\Delta E|,\alpha,\frac{L}{2}\right)-\mathfrak{h}\left(|\Delta E|,\alpha,z_0,\frac{L}{2}\right)\right\}\left(1+\frac{1}{\exp\left(2\pi|\Delta E|/\alpha\right)-1}\right)\right.$$

$$\left. +\theta(\Delta E)\left\{\frac{\Delta E}{2\pi}+\mathfrak{f}\left(\Delta E,\alpha,\frac{L}{2}\right)-\mathfrak{h}\left(\Delta E,\alpha,z_0,\frac{L}{2}\right)\right\}\left(\frac{1}{\exp\left(2\pi\Delta E/\alpha\right)-1}\right)\right] \qquad (B2)$$

where we have defined

$$\mathfrak{f}\left(\Delta E, \alpha, \frac{L}{2}\right) = 2\sum_{n=1}^{\infty} \mathfrak{g}\left(\Delta E, \alpha, \frac{nL}{2}\right) \qquad \text{(B3)}$$

$$\mathfrak{h}\left(\Delta E, \alpha, z_0, \frac{L}{2}\right) = \sum_{n=-\infty}^{\infty} \mathfrak{g}\left(\Delta E, \alpha, z_0 - \frac{nL}{2}\right) \qquad \text{(B4)}$$

where $\mathfrak{g}(\Delta E, \alpha, z_0)$ is defined as

$$\mathfrak{g}(\Delta E, \alpha, z_0) = \frac{\sin(\frac{2\Delta E}{\alpha}\sinh^{-1}(\alpha z_0))}{4\pi z_0\sqrt{1 + \alpha^2 z_0^2}}. \qquad \text{(B5)}$$

APPENDIX C: THERMAL WIGHTMAN FUNCTION OF A SINGLE ATOM IN EMPTY SPACE WITH RESPECT TO A COACCELERATED OBSERVER

In this Appendix, we present some of the intermediate steps leading to thermal Wightman function Eq. (36). Using Eq. (27) in Eq. (32), the thermal Wightman function takes the following form for an arbitrary temperature T,

$$G_\beta^+(x(\tau), x(\tau')) = \int_0^\infty d\omega \int_{-\infty}^\infty dk_y \int_{-\infty}^\infty dk_z \left[\sum_{\sigma=0}^\infty (\sigma + 1)e^{-\beta\omega\sigma}\mathcal{V}_{\omega,k_y,k_z}(\tau, \mathbf{x})\mathcal{V}_{\omega,k_y,k_z}^\star(\tau', \mathbf{x}')\right.$$

$$\left. + \sum_{\sigma=1}^\infty \sigma e^{-\beta\omega\sigma}\mathcal{V}_{\omega,k_y,k_z}^\star(\tau, \mathbf{x})\mathcal{V}_{\omega,k_y,k_z}(\tau', \mathbf{x}')\right] \Big/ \sum_{\sigma=0}^\infty e^{-\beta\omega\sigma}$$

$$= \int_0^\infty d\omega \int_{-\infty}^\infty dk_y \int_{-\infty}^\infty dk_z \left[\frac{e^{\omega/T}}{e^{\omega/T} - 1}\mathcal{V}_{\omega,k_y,k_z}(\tau, \mathbf{x})\mathcal{V}_{\omega,k_y,k_z}^\star(\tau', \mathbf{x}')\right.$$

$$\left. + \frac{1}{e^{\omega/T} - 1}\mathcal{V}_{\omega,k_y,k_z}^\star(\tau, \mathbf{x})\mathcal{V}_{\omega,k_y,k_z}(\tau', \mathbf{x}')\right]. \qquad \text{(C1)}$$

Using Eqs. (28) and (35) in Eq. (C1), the above result simplifies to the form

$$G_\beta^+(x(\tau), x(\tau')) = \frac{1}{4\pi^4\alpha}\int_0^\infty d\omega \int_{-\infty}^\infty dk_y \int_{-\infty}^\infty dk_z \sinh\left(\frac{\pi\omega}{\alpha}\right)\mathcal{K}_{i\omega/\alpha}^2\left(\frac{k_\perp}{\alpha}\right)\left[\frac{e^{\omega/T}}{e^{\omega/T} - 1}e^{-i\omega(\tau-\tau')} + \frac{1}{e^{\omega/T} - 1}e^{i\omega(\tau-\tau')}\right] \qquad \text{(C2)}$$

$$= \frac{1}{4\pi^2}\int_0^\infty d\omega\,\omega\left[\frac{e^{\omega/T}}{e^{\omega/T} - 1}e^{-i\omega(\tau-\tau')} + \frac{1}{e^{\omega/T} - 1}e^{i\omega(\tau-\tau')}\right]$$

$$= -\frac{1}{4\pi^2}\sum_{s=-\infty}^\infty \frac{1}{(\Delta\tau - is\beta - i\varepsilon)^2} \qquad \text{(C3)}$$

where in the second line, we have used the integral

$$\int_{-\infty}^\infty dk_y \int_{-\infty}^\infty dk_z \mathcal{K}_{i\omega/\alpha}^2\left(\frac{k_\perp}{\alpha}\right) = \frac{\alpha\pi^2\omega}{\sinh(\pi\omega/\alpha)}. \qquad \text{(C4)}$$

APPENDIX D: THERMAL WIGHTMAN FUNCTION OF A SINGLE ATOM IN CAVITY WITH RESPECT TO A COACCELERATED OBSERVER

In this Appendix, we present some of the intermediate steps leading to thermal Wightman function Eq. (40).

In the presence of a single reflecting boundary, the Rindler counterpart of the scalar field operator [Eq. (27)]

obeys the Dirichlet boundary condition $\phi|_{z=0} = 0$. The positive frequency Rindler mode function for the massless scalar field takes the form [39]

$$\mathcal{V}_{\omega,k_y,k_z}(\tau, \mathbf{x}) = \sqrt{\frac{\sinh(\pi\omega/\alpha)}{2\pi^4\alpha}}\mathcal{K}_{i\frac{\omega}{\alpha}}\left(\frac{k_\perp}{\alpha}e^{\alpha\eta}\right)$$

$$\times \sin(k_z z)e^{-i\omega\tau + ik_y y}. \qquad \text{(D1)}$$

Inserting Eq. (D1) in Eq. (C1), the thermal Wightman function takes the form

$$G_\beta^+(x(\tau), x(\tau')) = \frac{1}{4\pi^4\alpha} \int_0^\infty d\omega \int_{-\infty}^\infty dk_y \int_{-\infty}^\infty dk_z \sinh\left(\frac{\pi\omega}{\alpha}\right) \mathcal{K}_{i\omega/\alpha}\left(\frac{k_\perp}{\alpha} e^{\alpha\eta}\right) \mathcal{K}_{i\omega/\alpha}\left(\frac{k_\perp}{\alpha} e^{\alpha\eta'}\right) \{\cos[k_z(z - z')]$$
$$- \cos[k_z(z + z')]\} \times \left[\frac{e^{\omega/T}}{e^{\omega/T} - 1} e^{-i\omega(\tau-\tau')+ik_y(y-y')} + \frac{1}{e^{\omega/T} - 1} e^{i\omega(\tau-\tau')-ik_y(y-y')}\right]. \tag{D2}$$

Now for the cavity scenario, the Dirichlet boundary condition obeyed by the scalar field is $\phi|_{z=0} = \phi|_{z=L} = 0$. Using the above boundary condition [Eq. (D2)] and by using the method of images, the thermal Wightman function of the massless scalar field confined to the cavity turns out to be

$$G_\beta^+(x(\tau), x(\tau')) = \frac{1}{4\pi^4\alpha} \sum_{n=-\infty}^\infty \int_0^\infty d\omega \int_{-\infty}^\infty dk_y \int_{-\infty}^\infty dk_z \sinh\left(\frac{\pi\omega}{\alpha}\right) \mathcal{K}_{i\omega/\alpha}\left(\frac{k_\perp}{\alpha} e^{\alpha\eta}\right) \mathcal{K}_{i\omega/\alpha}\left(\frac{k_\perp}{\alpha} e^{\alpha\eta'}\right)$$
$$\times \{\cos[k_z(z - z' - nL)] - \cos[k_z(z + z' - nL)]\} \left[\frac{e^{\omega/T}}{e^{\omega/T} - 1} e^{-i\omega(\tau-\tau')+ik_y(y-y')}\right.$$
$$\left. + \frac{1}{e^{\omega/T} - 1} e^{i\omega(\tau-\tau')-ik_y(y-y')}\right]. \tag{D3}$$

Inserting the atomic trajectory Eq. (39) in Eq. (D3), along with the result [39]

$$\int_{-\infty}^\infty dk_y \int_{-\infty}^\infty dk_z \mathcal{K}_{i\omega/\alpha}^2\left(\frac{k_\perp}{\alpha}\right) \cos\left[2k_z\frac{d}{2}\right] = \frac{\alpha\pi^2}{\sinh(\pi\omega/\alpha)} \frac{\sin\left(\frac{2\omega}{\alpha}\sinh^{-1}\left(\frac{d\alpha}{2}\right)\right)}{d\sqrt{1 + \frac{1}{4}\alpha^2 d^2}}, \tag{D4}$$

and following the procedure in Appendix C, the thermal Wightman function inside the cavity becomes

$$G_\beta^+(x(\tau), x(\tau')) = -\frac{1}{4\pi^2} \sum_{n=-\infty}^\infty \sum_{s=-\infty}^\infty \left[\frac{\mathcal{B}_1}{\mathcal{C}_1} \frac{1}{(\Delta\tau - is\beta - i\varepsilon)^2 - \mathcal{B}_1^2} - \frac{\mathcal{B}_2}{\mathcal{C}_2} \frac{1}{(\Delta\tau - is\beta - i\varepsilon)^2 - \mathcal{B}_2^2}\right] \tag{D5}$$

with

$$\mathcal{B}_1 = \frac{2}{\alpha}\sinh^{-1}\left(\frac{nL\alpha}{2}\right), \qquad \mathcal{C}_1 = nL\sqrt{1 + \frac{1}{4}\alpha^2 n^2 L^2}$$
$$\mathcal{B}_2 = \frac{2}{\alpha}\sinh^{-1}\left(\alpha\left(z_0 - \frac{nL}{2}\right)\right), \qquad \mathcal{C}_2 = (2z_0 - nL)\sqrt{1 + \frac{1}{4}\alpha^2(2z_0 - nL)^2}. \tag{D6}$$

APPENDIX E: TRANSITION RATES OF TWO ATOMS IN EMPTY SPACE WITH RESPECT TO A LOCAL INERTIAL OBSERVER

In this Appendix, we present some of the intermediate steps leading to Eqs. (57) and (58). The form of the Wightman functions for the trajectories of the two atoms are given in Eqs. (55) and (56). Substituting this forms into Eq. (48) and Eq. (51), the transition rate of the two-atom system from the initial state $|\psi\rangle$ to the final state $|E_n\rangle$ can be expressed as

$$\mathcal{R}_{|\psi\rangle \to |E_n\rangle} = \lambda^2[|m_{E_n\psi}^{(A)}|^2 \mathcal{F}_{AA}(\Delta E) + |m_{E_n\psi}^{(B)}|^2 \mathcal{F}_{BB}(\Delta E) + m_{E_n\psi}^{(B)} m_{E_n\psi}^{(A)*} \mathcal{F}_{AB}(\Delta E) + m_{E_n\psi}^{(A)} m_{E_n\psi}^{(B)*} \mathcal{F}_{BA}(\Delta E)] \tag{E1}$$

with

$$\mathcal{F}_{\xi\xi'}(\Delta E) = -\frac{\alpha^2}{16\pi^2} \int_{-\infty}^{+\infty} d(\Delta\tau) e^{-i\Delta E\Delta\tau} \frac{1}{\sinh^2\left[\frac{1}{2}(\alpha\Delta\tau - i\varepsilon)\right]} \tag{E2}$$

for $\xi = \xi'$ and

$$\mathcal{F}_{\xi\xi'}(\Delta E) = -\frac{\alpha^2}{16\pi^2} \int_{-\infty}^{+\infty} d(\Delta\tau) e^{-i\Delta E\Delta\tau} \frac{1}{\sinh^2[\frac{1}{2}(\alpha\Delta\tau - i\varepsilon)] - \frac{1}{4}d^2\alpha^2} \tag{E3}$$

for $\xi \neq \xi'$. We simplify the transition rate Eq. (E1) by performing contour integration, leading to

$$\mathcal{R}_{|\psi\rangle\to|E_n\rangle} = \lambda^2 \left\{ \theta(-\Delta E) \left(\frac{|\Delta E|}{2\pi} + \frac{\sin 2\theta \sin(\frac{2|\Delta E|}{\alpha}\sinh^{-1}(\frac{1}{2}\alpha d))}{2\pi d\sqrt{1 + \frac{1}{4}d^2\alpha^2}} \right) \left(1 + \frac{1}{e^{2\pi|\Delta E|/\alpha} - 1} \right) \right.$$

$$\left. + \theta(\Delta E) \left(\frac{\Delta E}{2\pi} + \frac{\sin 2\theta \sin(\frac{2\Delta E}{\alpha}\sinh^{-1}(\frac{1}{2}\alpha d))}{2\pi d\sqrt{1 + \frac{1}{4}d^2\alpha^2}} \right) \left(\frac{1}{e^{2\pi\Delta E/\alpha} - 1} \right) \right\} \tag{E4}$$

where $\theta(\Delta E)$ is defined in Eq. (15).

APPENDIX F: TRANSITION RATES OF TWO ATOMS IN A CAVITY WITH RESPECT TO A LOCAL INERTIAL OBSERVER

In this Appendix, we present some of the intermediate steps leading to Eqs. (63) and (64). The form of the Wightman functions for the trajectories of the two atoms are given in Eqs. (61) and (62). Substituting this forms into Eqs. (48) and (51), the transition rate of the two-atom system from the initial state $|\psi\rangle$ to the final state $|E_n\rangle$ can be expressed as

$$\mathcal{R}_{|\psi\rangle\to|E_n\rangle} = \lambda^2 \sum_{n=-\infty}^{\infty} [|m_{E_n\psi}^{(A)}|^2 \mathcal{F}_{AA}(\Delta E) + |m_{E_n\psi}^{(B)}|^2 \mathcal{F}_{BB}(\Delta E) + m_{E_n\psi}^{(B)} m_{E_n\psi}^{(A)*} \mathcal{F}_{AB}(\Delta E) + m_{E_n\psi}^{(A)} m_{E_n\psi}^{(B)*} \mathcal{F}_{BA}(\Delta E)] \tag{F1}$$

with

$$\mathcal{F}_{\xi\xi'}(\Delta E) = -\frac{\alpha^2}{16\pi^2} \int_{-\infty}^{+\infty} d(\Delta\tau) e^{-i\Delta E\Delta\tau} \left[\frac{1}{\sinh^2[\frac{1}{2}(\alpha\Delta\tau - i\varepsilon)] - \frac{1}{4}d_1^2\alpha^2} - \frac{1}{\sinh^2[\frac{1}{2}(\alpha\Delta\tau - i\varepsilon)] - \frac{1}{4}d_2^2\alpha^2} \right] \tag{F2}$$

for $\xi = \xi'$ and

$$\mathcal{F}_{\xi\xi'}(\Delta E) = -\frac{\alpha^2}{16\pi^2} \int_{-\infty}^{+\infty} d(\Delta\tau) e^{-i\Delta E\Delta\tau} \left[\frac{1}{\sinh^2[\frac{1}{2}(\alpha\Delta\tau - i\varepsilon)] - \frac{1}{4}d_3^2\alpha^2} - \frac{1}{\sinh^2[\frac{1}{2}(\alpha\Delta\tau - i\varepsilon)] - \frac{1}{4}d_4^2\alpha^2} \right] \tag{F3}$$

for $\xi \neq \xi'$. Equation (F1) can be further simplified by performing contour integration to obtain

$$\mathcal{R}_{|\psi\rangle\to|E_n\rangle} = \lambda^2 \left\{ \theta(-\Delta E) \left(\frac{|\Delta E|}{2\pi} + \mathfrak{f}\left(|\Delta E|, \alpha, \frac{L}{2}\right) - \cos^2\theta \mathfrak{h}\left(|\Delta E|, \alpha, z_0, \frac{L}{2}\right) - \sin^2\theta \mathfrak{m}\left(|\Delta E|, \alpha, z_0, d, \frac{L}{2}\right) \right. \right.$$

$$\left. + \sin 2\theta \mathfrak{n}\left(|\Delta E|, \alpha, \frac{d}{2}, \frac{L}{2}\right) - \sin 2\theta \mathfrak{m}\left(|\Delta E|, \alpha, z_0, \frac{d}{2}, \frac{L}{2}\right) \right) \left(1 + \frac{1}{\exp(2\pi|\Delta E|/\alpha) - 1} \right)$$

$$+ \theta(\Delta E) \left(\frac{\Delta E}{2\pi} + \mathfrak{f}\left(\Delta E, \alpha, \frac{L}{2}\right) - \cos^2\theta \mathfrak{h}\left(\Delta E, \alpha, z_0, \frac{L}{2}\right) - \sin^2\theta \mathfrak{m}\left(\Delta E, \alpha, z_0, d, \frac{L}{2}\right) \right.$$

$$\left. \left. + \sin 2\theta \mathfrak{n}\left(\Delta E, \alpha, \frac{d}{2}, \frac{L}{2}\right) - \sin 2\theta \mathfrak{m}\left(\Delta E, \alpha, z_0, \frac{d}{2}, \frac{L}{2}\right) \right) \left(\frac{1}{\exp(2\pi\Delta E/\alpha) - 1} \right) \right\} \tag{F4}$$

where we have defined

$$\mathfrak{m}\left(\Delta E, \alpha, z_0, d, \frac{L}{2}\right) = \sum_{n=-\infty}^{\infty} \mathfrak{g}\left(\Delta E, \alpha, z_0 + d - \frac{nL}{2}\right) \tag{F5}$$

$$\mathfrak{n}\left(\Delta E, \alpha, \frac{d}{2}, \frac{L}{2}\right) = \sum_{n=-\infty}^{\infty} \mathfrak{g}\left(\Delta E, \alpha, \frac{d - nL}{2}\right) \tag{F6}$$

and $\mathfrak{g}(\Delta E, \alpha, z_0)$ is defined in Appendix B.

APPENDIX G: THERMAL WIGHTMAN FUNCTION OF TWO ATOMS IN EMPTY SPACE WITH RESPECT TO A COACCELERATED OBSERVER

In this Appendix, we present some of the intermediate steps leading to thermal Wightman functions Eqs. (77) and (78). Using Eq. (68) in Eq. (73), the thermal Wightman function takes the following form for an arbitrary temperature T

$$
\begin{aligned}
G_\beta^+(x_\xi(\tau), x_{\xi'}(\tau')) &= \int_0^\infty d\omega \int_{-\infty}^\infty dk_y \int_{-\infty}^\infty dk_z \left[\sum_{\sigma=0}^\infty (\sigma+1) e^{-\beta\omega\sigma} \mathcal{V}_{\omega,k_y,k_z}(\tau_\xi, \mathbf{x}_\xi) \mathcal{V}_{\omega,k_y,k_z}^\star(\tau'_{\xi'}, \mathbf{x}'_{\xi'}) \right. \\
&\quad \left. + \sum_{\sigma=1}^\infty \sigma e^{-\beta\omega\sigma} \mathcal{V}_{\omega,k_y,k_z}^\star(\tau_\xi, \mathbf{x}_\xi) \mathcal{V}_{\omega,k_y,k_z}(\tau'_{\xi'}, \mathbf{x}'_{\xi'}) \right] \Big/ \sum_{\sigma=0}^\infty e^{-\beta\omega\sigma} \\
&= \int_0^\infty d\omega \int_{-\infty}^\infty dk_y \int_{-\infty}^\infty dk_z \left[\frac{e^{\omega/T}}{e^{\omega/T} - 1} \mathcal{V}_{\omega,k_y,k_z}(\tau_\xi, \mathbf{x}_\xi) \mathcal{V}_{\omega,k_y,k_z}^\star(\tau'_{\xi'}, \mathbf{x}'_{\xi'}) \right. \\
&\quad \left. + \frac{1}{e^{\omega/T} - 1} \mathcal{V}_{\omega,k_y,k_z}^\star(\tau_\xi, \mathbf{x}_\xi) \mathcal{V}_{\omega,k_y,k_z}(\tau'_{\xi'}, \mathbf{x}'_{\xi'}) \right]
\end{aligned}
\tag{G1}
$$

Inserting Eqs. (69) and (76) in Eq. (G1), the above result simplifies to the form

$$
G_\beta^+(x_\xi(\tau), x_{\xi'}(\tau')) = \frac{1}{4\pi^4\alpha} \int_0^\infty d\omega \int_{-\infty}^\infty dk_y \int_{-\infty}^\infty dk_z \sinh\left(\frac{\pi\omega}{\alpha}\right) \mathcal{K}_{i\omega/\alpha}^2\left(\frac{k_\perp}{\alpha}\right) \left[\frac{e^{\omega/T}}{e^{\omega/T} - 1} e^{-i\omega(\tau-\tau')} + \frac{1}{e^{\omega/T} - 1} e^{i\omega(\tau-\tau')} \right]. \tag{G2}
$$

Now, using Eq. (C4) and the integral

$$
\int_{-\infty}^\infty dk_y \int_{-\infty}^\infty dk_z \mathcal{K}_{i\omega/\alpha}^2\left(\frac{k_\perp}{\alpha}\right) e^{-ik_z d} = \frac{\alpha\pi^2}{\sinh(\pi\omega/\alpha)} \frac{\sin\left(\frac{2\omega}{\alpha}\sinh^{-1}\left(\frac{d\alpha}{2}\right)\right)}{d\sqrt{1+\frac{1}{4}\alpha^2 d^2}} \tag{G3}
$$

the thermal Wightman function takes the form

$$
G_\beta^+(x_\xi(\tau), x_{\xi'}(\tau')) = -\frac{1}{4\pi^2} \sum_{s=-\infty}^\infty \frac{1}{(\Delta\tau - is\beta - i\varepsilon)^2} \tag{G4}
$$

for $\xi = \xi'$, and

$$
G_\beta^+(x_\xi(\tau), x_{\xi'}(\tau')) = -\frac{\mathcal{B}}{4\pi^2\mathcal{C}} \sum_{s=-\infty}^\infty \frac{1}{(\Delta\tau - is\beta - i\varepsilon)^2 - \mathcal{B}^2} \tag{G5}
$$

for $\xi \neq \xi'$, with $\mathcal{B} = \frac{2}{\alpha}\sinh^{-1}\left(\frac{d\alpha}{2}\right)$ and $\mathcal{C} = d\sqrt{1+\frac{1}{4}\alpha^2 d^2}$.

APPENDIX H: THERMAL WIGHTMAN FUNCTION OF TWO ATOMS IN CAVITY WITH RESPECT TO A COACCELERATED OBSERVER

In this Appendix, we present some of the intermediate steps leading to thermal Wightman functions Eqs. (82) and (83).

Considering that the Rindler counterpart of the scalar field Eq. (68) obeys the Dirichlet boundary condition $\phi|_{z=0} = \phi|_{z=L} = 0$, and by following a similar method we have used for the single atom case, the positive frequency thermal Wightmann function of the massless scalar field confined in the cavity turns out to be

$$G_\beta^+(x_\xi(\tau), x_{\xi'}(\tau')) = \frac{1}{4\pi^4 \alpha} \sum_{n=-\infty}^{\infty} \int_0^\infty d\omega \int_{-\infty}^\infty dk_y \int_{-\infty}^\infty dk_z \sinh\left(\frac{\pi\omega}{\alpha}\right) \mathcal{K}_{i\omega/\alpha}\left(\frac{k_\perp}{\alpha} e^{\alpha\eta_\xi}\right) \mathcal{K}_{i\omega/\alpha}\left(\frac{k_\perp}{\alpha} e^{\alpha\eta'_{\xi'}}\right)$$

$$\times \left\{\cos[k_z(z_\xi - z'_{\xi'} - nL)] - \cos[k_z(z_\xi + z'_{\xi'} - nL)]\right\} \left[\frac{e^{\omega/T}}{e^{\omega/T} - 1} e^{-i\omega(\tau_\xi - \tau'_{\xi'}) + ik_y(y_\xi - y'_{\xi'})}\right.$$

$$\left. + \frac{1}{e^{\omega/T} - 1} e^{i\omega(\tau_\xi - \tau'_{\xi'}) - ik_y(y_\xi - y'_{\xi'})}\right]. \tag{H1}$$

Inserting the atomic trajectories Eq. (81) in Eq. (H1) and following the procedure in Appendix D, above result simplifies to the form

$$G_\beta^+(x_\xi(\tau), x_{\xi'}(\tau')) = -\frac{1}{4\pi^2} \sum_{n=-\infty}^{\infty} \sum_{s=-\infty}^{\infty} \left[\frac{\mathcal{B}_1}{\mathcal{C}_1} \frac{1}{(\Delta\tau - is\beta - i\epsilon)^2 - \mathcal{B}_1^2} - \frac{\mathcal{B}_3}{\mathcal{C}_3} \frac{1}{(\Delta\tau - is\beta - i\epsilon)^2 - \mathcal{B}_3^2}\right] \tag{H2}$$

for $\xi = \xi'$ with $\mathcal{B}_1, \mathcal{C}_1$ are given in Eq. (D6), $\mathcal{B}_3 = \frac{2}{\alpha}\sinh^{-1}\left(\alpha(z_\xi - \frac{nL}{2})\right)$, $\mathcal{C}_3 = (2z_\xi - nL)\sqrt{1 + \frac{1}{4}\alpha^2(2z_\xi - nL)^2}$ and

$$G_\beta^+(x_\xi(\tau), x_{\xi'}(\tau')) = -\frac{1}{4\pi^2} \sum_{n=-\infty}^{\infty} \sum_{s=-\infty}^{\infty} \left[\frac{\mathcal{B}_4}{\mathcal{C}_4} \frac{1}{(\Delta\tau - is\beta - i\epsilon)^2 - \mathcal{B}_4^2} - \frac{\mathcal{B}_5}{\mathcal{C}_5} \frac{1}{(\Delta\tau - is\beta - i\epsilon)^2 - \mathcal{B}_5^2}\right] \tag{H3}$$

for $\xi \neq \xi'$ with $\{\mathcal{B}_4 = -\frac{2}{\alpha}\sinh^{-1}(\frac{(d+nL)\alpha}{2}), \mathcal{C}_4 = -(d+nL)\sqrt{1 + \frac{1}{4}\alpha^2(d+nL)^2}\}$ (for $\xi = A, \xi' = B$), $\{\mathcal{B}_4 = \frac{2}{\alpha}\sinh^{-1}(\frac{(d-nL)\alpha}{2})$, $\mathcal{C}_4 = (d-nL)\sqrt{1 + \frac{1}{4}\alpha^2(d-nL)^2}\}$ (for $\xi = B, \xi' = A$), $\mathcal{B}_5 = \frac{2}{\alpha} \times \sinh^{-1}(\alpha(z_0 + \frac{d-nL}{2}))$, and $\mathcal{C}_5 = (2z_0 + d - nL) \times \sqrt{1 + \frac{1}{4}\alpha^2(2z_0 + d - nL)^2}$.

---

[1] I. Fuentes-Schuller and R. B. Mann, Alice falls into a black hole: Entanglement in noninertial frames, Phys. Rev. Lett. **95**, 120404 (2005).

[2] B. Richter and Y. Omar, Degradation of entanglement between two accelerated parties: Bell states under the Unruh effect, Phys. Rev. A **92**, 022334 (2015).

[3] P. M. Alsing, I. Fuentes-Schuller, R. B. Mann, and T. E. Tessier, Entanglement of Dirac fields in noninertial frames, Phys. Rev. A **74**, 032326 (2006).

[4] A. Bermudez and M. A. Martin-Delgado, Hyper-entanglement in a relativistic two-body system, J. Phys. A **41**, 485302 (2008).

[5] M.-R. Hwang, E. Jung, and D. Park, Three-tangle in non-inertial frame, Classical Quantum Gravity **29**, 224004 (2012).

[6] M.-R. Hwang, D. Park, and E. Jung, Tripartite entanglement in a noninertial frame, Phys. Rev. A **83**, 012111 (2011).

[7] E. Hagley, X. Maître, G. Nogues, C. Wunderlich, M. Brune, J. M. Raimond, and S. Haroche, Generation of Einstein-Podolsky-Rosen pairs of atoms, Phys. Rev. Lett. **79**, 1 (1997).

[8] M. B. Plenio, S. F. Huelga, A. Beige, and P. L. Knight, Cavity-loss-induced generation of entangled atoms, Phys. Rev. A **59**, 2468 (1999).

[9] L. Amico, R. Fazio, A. Osterloh, and V. Vedral, Entanglement in many-body systems, Rev. Mod. Phys. **80**, 517 (2008).

[10] G. S. Agarwal, Quantum-entanglement-initiated super Raman scattering, Phys. Rev. A **83**, 023802 (2011).

[11] B. Reznik, Entanglement from the vacuum, Found. Phys. **33**, 167 (2003).

[12] B. Reznik, A. Retzker, and J. Silman, Violating Bell's inequalities in vacuum, Phys. Rev. A **71**, 042104 (2005).

[13] D. Braun, Entanglement from thermal blackbody radiation, Phys. Rev. A **72**, 062324 (2005).

[14] S. Massar and P. Spindel, Einstein-Podolsky-Rosen correlations between two uniformly accelerated oscillators, Phys. Rev. D **74**, 085031 (2006).

[15] J. Franson, Generation of entanglement outside of the light cone, J. Mod. Opt. **55**, 2117 (2008).

[16] S.-Y. Lin and B. L. Hu, Temporal and spatial dependence of quantum entanglement from a field theory perspective, Phys. Rev. D **79**, 085020 (2009).

[17] S.-Y. Lin and B. L. Hu, Entanglement creation between two causally disconnected objects, Phys. Rev. D **81**, 045019 (2010).

[18] G. Menezes, Radiative processes of two entangled atoms outside a Schwarzschild black hole, Phys. Rev. D **94**, 105008 (2016).

[19] S. Sen, R. Mandal, and S. Gangopadhyay, Equivalence principle and HBAR entropy of an atom falling into a quantum corrected black hole, Phys. Rev. D **105,** 085007 (2022).

[20] S. Sen, R. Mandal, and S. Gangopadhyay, Near horizon aspects of acceleration radiation of an atom falling into a class of static spherically symmetric black hole geometries, Phys. Rev. D **106,** 025004 (2022).

[21] S. Sen, R. Mandal, and S. Gangopadhyay, Near horizon approximation and beyond for a two-level atom falling into a Kerr-Newman black hole, Eur. Phys. J. Plus **138,** 855 (2023).

[22] S. A. Fulling, Nonuniqueness of canonical field quantization in Riemannian space-time, Phys. Rev. D **7,** 2850 (1973).

[23] P. C. W. Davies, Scalar production in Schwarzschild and Rindler metrics, J. Phys. A **8,** 609 (1975).

[24] W. G. Unruh, Experimental black-hole evaporation?, Phys. Rev. Lett. **46,** 1351 (1981).

[25] N. D. Birrell and P. Davies, *Quantum Fields in Curved Space* (Cambridge University Press, Cambridge, England, 1984), 10.1017/CBO9780511622632.

[26] V. Frolov and V. Ginzburg, Excitation and radiation of an accelerated detector and anomalous doppler effect, Phys. Lett. **116A,** 423 (1986).

[27] A. Higuchi and G. E. A. Matsas, Fulling-Davies-Unruh effect in classical field theory, Phys. Rev. D **48,** 689 (1993).

[28] O. Levin, Y. Peleg, and A. Peres, Quantum detector in an accelerated cavity, J. Phys. A **25,** 6471 (1992).

[29] J. Audretsch and R. Müller, Spontaneous excitation of an accelerated atom: The contributions of vacuum fluctuations and radiation reaction, Phys. Rev. A **50,** 1755 (1994).

[30] J. Audretsch and R. Müller, Radiative energy shifts of an accelerated two-level system, Phys. Rev. A **52,** 629 (1995).

[31] R. Passante, Radiative level shifts of an accelerated hydrogen atom and the Unruh effect in quantum electrodynamics, Phys. Rev. A **57,** 1590 (1998).

[32] D. A. T. Vanzella and G. E. A. Matsas, Decay of accelerated protons and the existence of the Fulling-Davies-Unruh effect, Phys. Rev. Lett. **87,** 151301 (2001).

[33] D. T. Alves and L. C. B. Crispino, Response rate of a uniformly accelerated source in the presence of boundaries, Phys. Rev. D **70,** 107703 (2004).

[34] H. Yu and S. Lu, Spontaneous excitation of an accelerated atom in a spacetime with a reflecting plane boundary, Phys. Rev. D **72,** 064022 (2005).

[35] H. Yu and S. Lu, Erratum: Spontaneous excitation of an accelerated atom in a spacetime with a reflecting plane boundary [Phys. Rev. D **72,** 064022 (2005)], Phys. Rev. D **73,** 109901(E) (2006).

[36] Z. Zhu, H. Yu, and S. Lu, Spontaneous excitation of an accelerated hydrogen atom coupled with electromagnetic vacuum fluctuations, Phys. Rev. D **73,** 107501 (2006).

[37] H. Yu and Z. Zhu, Spontaneous absorption of an accelerated hydrogen atom near a conducting plane in vacuum, Phys. Rev. D **74,** 044032 (2006).

[38] S.-Y. Lin and B. L. Hu, Accelerated detector-quantum field correlations: From vacuum fluctuations to radiation flux, Phys. Rev. D **73,** 124018 (2006).

[39] Z. Zhu and H. Yu, Fulling–Davies–Unruh effect and spontaneous excitation of an accelerated atom interacting with a quantum scalar field, Phys. Lett. B **645,** 459 (2007).

[40] W. Zhou and H. Yu, Spontaneous excitation of a uniformly accelerated atom coupled to vacuum Dirac field fluctuations, Phys. Rev. A **86,** 033841 (2012).

[41] Z. Zhi-Ying and Y. Hong-Wei, Accelerated multi-level atoms in an electromagnetic vacuum and Fulling–Davies–Unruh effect, Chin. Phys. Lett. **25,** 1575 (2008).

[42] L. C. B. Crispino, A. Higuchi, and G. E. A. Matsas, Interaction of Hawking radiation and a static electric charge, Phys. Rev. D **58,** 084027 (1998).

[43] D. Marolf, D. Minic, and S. F. Ross, Notes on spacetime thermodynamics and the observer dependence of entropy, Phys. Rev. D **69,** 064006 (2004).

[44] G. E. A. Matsas and A. R. R. da Silva, New thought experiment to test the generalized second law of thermodynamics, Phys. Rev. D **71,** 107501 (2005).

[45] A. Noto and R. Passante, van der Waals interaction energy between two atoms moving with uniform acceleration, Phys. Rev. D **88,** 025041 (2013).

[46] J. Marino, A. Noto, and R. Passante, Thermal and nonthermal signatures of the Unruh effect in Casimir-Polder forces, Phys. Rev. Lett. **113,** 020403 (2014).

[47] L. Rizzuto, M. Lattuca, J. Marino, A. Noto, S. Spagnolo, W. Zhou, and R. Passante, Nonthermal effects of acceleration in the resonance interaction between two uniformly accelerated atoms, Phys. Rev. A **94,** 012121 (2016).

[48] W. Zhou, R. Passante, and L. Rizzuto, Resonance interaction energy between two accelerated identical atoms in a coaccelerated frame and the Unruh effect, Phys. Rev. D **94,** 105025 (2016).

[49] G. Fiscelli, L. Rizzuto, and R. Passante, Resonance energy transfer between two atoms in a conducting cylindrical waveguide, Phys. Rev. A **98,** 013849 (2018).

[50] G. Menezes and N. F. Svaiter, Radiative processes of uniformly accelerated entangled atoms, Phys. Rev. A **93,** 052117 (2016).

[51] M. S. Soares, N. F. Svaiter, C. A. D. Zarro, and G. Menezes, Uniformly accelerated quantum counting detector in Minkowski and Fulling vacuum states, Phys. Rev. A **103,** 042225 (2021).

[52] W. Zhou, L. Rizzuto, and R. Passante, Vacuum fluctuations and radiation reaction contributions to the resonance dipole-dipole interaction between two atoms near a reflecting boundary, Phys. Rev. A **97,** 042503 (2018).

[53] C. A. U. Lima, F. Brito, J. A. Hoyos, and D. A. T. Vanzella, Probing the Unruh effect with an accelerated extended system, Nat. Commun. **10,** 3030 (2019).

[54] J. D. Thompson, T. G. Tiecke, N. P. de Leon, J. Feist, A. V. Akimov, M. Gullans, A. S. Zibrov, V. Vuletić, and M. D. Lukin, Coupling a single trapped atom to a nanoscale optical cavity, Science **340,** 1202 (2013).

[55] P. Solano, J. A. Grover, J. E. Hoffman, S. Ravets, F. K. Fatemi, L. A. Orozco, and S. L. Rolston, *Chapter Seven— Optical Nanofibers: A New Platform for Quantum Optics* (Academic Press, New York, 2017), pp. 439–505.

[56] E. Vetsch, D. Reitz, G. Sagué, R. Schmidt, S. T. Dawkins, and A. Rauschenbeutel, Optical interface created by laser-cooled atoms trapped in the evanescent field surrounding an optical nanofiber, Phys. Rev. Lett. **104,** 203603 (2010).

[57] A. Goban, K. S. Choi, D. J. Alton, D. Ding, C. Lacroûte, M. Pototschnig, T. Thiele, N. P. Stern, and H. J. Kimble, Demonstration of a state-insensitive, compensated nanofiber trap, Phys. Rev. Lett. **109,** 033603 (2012).

[58] N. V. Corzo, J. Raskop, A. Chandra, A. S. Sheremet, B. Gouraud, and J. Laurat, Waveguide-coupled single collective excitation of atomic arrays, Nature (London) **566,** 359 (2019).

[59] D. E. Chang, J. S. Douglas, A. González-Tudela, C.-L. Hung, and H. J. Kimble, Colloquium: Quantum matter built from nanoscopic lattices of atoms and photons, Rev. Mod. Phys. **90,** 031002 (2018).

[60] N. Friis, A. R. Lee, K. Truong, C. Sabín, E. Solano, G. Johansson, and I. Fuentes, Relativistic quantum teleportation with superconducting circuits, Phys. Rev. Lett. **110,** 113602 (2013).

[61] S. Felicetti, C. Sabín, I. Fuentes, L. Lamata, G. Romero, and E. Solano, Relativistic motion with superconducting qubits, Phys. Rev. B **92,** 064501 (2015).

[62] Z. Huang and H. Situ, Protection of quantum dialogue affected by quantum field, Quantum Inf. Process. **18,** 37 (2019).

[63] Z. Huang and Z. He, Deterministic secure quantum communication under vacuum fluctuation, Eur. Phys. J. D **74,** 176 (2020).

[64] M. R. R. Good, A. Lapponi, O. Luongo, and S. Mancini, Quantum communication through a partially reflecting accelerating mirror, Phys. Rev. D **104,** 105020 (2021).

[65] J. Åberg, S. Hengl, and R. Renner, Directed quantum communication, New J. Phys. **15,** 033025 (2013).

[66] J. Zhang and H. Yu, Unruh effect and entanglement generation for accelerated atoms near a reflecting boundary, Phys. Rev. D **75,** 104014 (2007).

[67] R. Zhou, R. O. Behunin, S.-Y. Lin, and B. Hu, Boundary effects on quantum entanglement and its dynamics in a detector-field system, J. High Energy Phys. 08 (2013) 040.

[68] S. Cheng, H. Yu, and J. Hu, Entanglement dynamics for uniformly accelerated two-level atoms in the presence of a reflecting boundary, Phys. Rev. D **98,** 025001 (2018).

[69] Z. Liu, J. Zhang, and H. Yu, Entanglement harvesting in the presence of a reflecting boundary, J. High Energy Phys. 08 (2021) 020.

[70] I. Akal, Y. Kusuki, N. Shiba, T. Takayanagi, and Z. Wei, Holographic moving mirrors, Classical Quantum Gravity **38,** 224001 (2021).

[71] R. Chatterjee, S. Gangopadhyay, and A. S. Majumdar, Resonance interaction of two entangled atoms accelerating between two mirrors, Eur. Phys. J. D **75,** 179 (2021).

[72] A. Mukherjee, S. Gangopadhyay, and A. S. Majumdar, Unruh quantum Otto engine in the presence of a reflecting boundary, J. High Energy Phys. 09 (2022) 105.

[73] S. Haroche and J.-M. Raimond, *Exploring the Quantum: Atoms, Cavities, and Photons* (Oxford University Press, New York, 2006).

[74] R. Chatterjee, S. Gangopadhyay, and A. S. Majumdar, Violation of equivalence in an accelerating atom-mirror system in the generalized uncertainty principle framework, Phys. Rev. D **104,** 124001 (2021).

[75] M. O. Scully, V. V. Kocharovsky, A. Belyanin, E. Fry, and F. Capasso, Enhancing acceleration radiation from

ground-state atoms via cavity quantum electrodynamics, Phys. Rev. Lett. **91,** 243004 (2003).

[76] A. Belyanin, V. V. Kocharovsky, F. Capasso, E. Fry, M. S. Zubairy, and M. O. Scully, Quantum electrodynamics of accelerated atoms in free space and in cavities, Phys. Rev. A **74,** 023807 (2006).

[77] G. A. Mourou, T. Tajima, and S. V. Bulanov, Optics in the relativistic regime, Rev. Mod. Phys. **78,** 309 (2006).

[78] U. Eichmann, T. Nubbemeyer, H. Rottke, and W. Sandner, Acceleration of neutral atoms in strong short-pulse laser fields, Nature (London) **461,** 1261 (2009).

[79] C. Maher-McWilliams, P. Douglas, and P. F. Barker, Laser-driven acceleration of neutral particles, Nat. Photonics **6,** 386 (2012).

[80] E. Arias, J. Dueñas, G. Menezes, and N. Svaiter, Boundary effects on radiative processes of two entangled atoms, J. High Energy Phys. 07 (**2016**) 147.

[81] C. Zhang and W. Zhou, Radiative processes of two accelerated entangled atoms near boundaries, Symmetry **11,** 1515 (2019).

[82] W. Zhou and H. Yu, Collective transitions of two entangled atoms and the Fulling-Davies-Unruh effect, Phys. Rev. D **101,** 085009 (2020).

[83] K. Lochan, H. Ulbricht, A. Vinante, and S. K. Goyal, Detecting acceleration-enhanced vacuum fluctuations with atoms inside a cavity, Phys. Rev. Lett. **125,** 241301 (2020).

[84] D. J. Stargen and K. Lochan, Cavity optimization for Unruh effect at small accelerations, Phys. Rev. Lett. **129,** 111303 (2022).

[85] N. Arya, V. Mittal, K. Lochan, and S. K. Goyal, Geometric phase assisted observation of noninertial cavity-QED effects, Phys. Rev. D **106,** 045011 (2022).

[86] B. F. Svaiter and N. F. Svaiter, Inertial and noninertial particle detectors and vacuum fluctuations, Phys. Rev. D **46,** 5267 (1992).

[87] M. E. Peskin, *An Introduction to Quantum Field Theory* (CRC Press, Boca Raton, 2018), 10.1201/9780429503559.

[88] E. Freitag and R. Busam, *Complex Analysis*, Universitext (Springer Berlin Heidelberg, Berlin, Heidelberg, 2009).

[89] J. Dalibard, J. Dupont-Roc, and C. Cohen-Tannoudji, Vacuum fluctuations and radiation reaction: Identification of their respective contributions, J. Phys. France **43,** 1617 (1982).

[90] J. Dalibard, J. Dupont-Roc, and C. Cohen-Tannoudji, Dynamics of a small system coupled to a reservoir: Reservoir fluctuations and self-reaction, J. Phys. France **45,** 637 (1984).

[91] J. E. Sansonetti, Wavelengths, transition probabilities, and energy levels for the spectra of rubidium, J. Phys. Chem. Ref. Data **35,** 301 (2006).

[92] C. Rodríguez-Camargo, G. Menezes, and N. Svaiter, Finite-time response function of uniformly accelerated entangled atoms, Ann. Phys. (Amsterdam) **396,** 266 (2018).

[93] M. Donaire, J. M. Muñoz Castañeda, and L. M. Nieto, Dipole-dipole interaction in cavity QED: The weak-coupling, non-degenerate regime, Phys. Rev. A **96,** 042714 (2017).

[94] I. S. Gradshteyn, I. M. Ryzhik, D. Zwillinger, and V. Moll, *Table of Integrals, Series, and Products*, 8th ed. (Academic Press, Amsterdam, 2014), https://cds.cern.ch/record/1702455.